Published in final edited form as:
Prog Retin Eye Res. 2012 March ; 31(2): 121–135. doi:10.1016/j.preteyeres.2011.12.001.

The Bisretinoids of Retinal Pigment Epithelium

Janet R. Sparrow[a,b,*], **Emily Gregory-Roberts**[a], **Kazunori Yamamoto**[a], **Anna Blonska**[a], **Shanti Kaligotla Ghosh**[a], **Keiko Ueda**[a], and **Jilin Zhou**[a]

[a]Department of Ophthalmology, Columbia University 10032

[b]Department of Pathology and Cell Biology, Columbia University 10032

Abstract

The retina exhibits an inherent autofluorescence that is imaged ophthalmoscopically as fundus autofluorescence. In clinical settings, fundus autofluorescence examination aids in the diagnosis and follow-up of many retinal disorders. Fundus autofluorescence originates from the complex mixture of bisretinoid fluorophores that are amassed by retinal pigment epithelial (RPE) cells as lipofuscin. Unlike the lipofuscin found in other cell-types, this material does not form as a result of oxidative stress. Rather, the formation is attributable to non-enzymatic reactions of vitamin A aldehyde in photoreceptor cells; transfer to RPE occurs upon phagocytosis of photoreceptor outer segments. These fluorescent pigments accumulate even in healthy photoreceptor cells and are generated as a consequence of the light capturing function of the cells. Nevertheless, the formation of this material is accelerated in some retinal disorders including recessive Stargardt disease and ELOVL-4-related retinal degeneration. As such, these bisretinoid side-products are implicated in the disease processes that threaten vision. In this article, we review our current understanding of the composition of RPE lipofuscin, the structural characteristics of the various bisretinoids, their related spectroscopic features and the biosynthetic pathways by which they form. We will revisit factors known to influence the extent of the accumulation and therapeutic strategies being used to limit bisretinoid formation. Given their origin from vitamin A aldehyde, an isomer of the visual pigment chromophore, it is not surprising that the bisretinoids of retina are light sensitive molecules. Accordingly, we will discuss recent findings that implicate the photodegradation of bisretinoid in the etiology of age-related macular degeneration.

Keywords

A2E; all-*trans*-retinal; bisretinoid; retinal pigment epithelium; macular degeneration; retina

1. The origin of RPE lipofuscin

The lipofuscin of retinal pigment epithelial (RPE) cells is amassed with age in organelles of the lysosomal compartment of the cells, in both healthy and diseased retina. It is generally agreed that this material originates, for the most part, from ingestion of shed photoreceptor outer segment membrane. Historically, however, opinions as to the molecular composition of RPE lipofuscin, have differed (Chio et al., 1969; Chio and Tappel, 1969; Chowdhury et

[*]Corresponding author: Dr. Janet R. Sparrow, Columbia University, Department of Ophthalmology, 630 W. 168[the] Streets, New York, NY 10032, Phone: 212-305-9944; Fax: 212-305-9638, jrs88@columbia.edu.

al., 2004; Eldred and Katz, 1991; Eldred and Katz, 1989), with one notion being that it consists of oxidatively modified lipid. Carboxyethyl pyrrole protein (CEP)-adducts, modifications that are generated from the oxidation of docosahexaenoate-containing lipids in photoreceptor cells have been detected in RPE lipofuscin (Ng et al., 2008). Presumably, the photooxidative process responsible for generating these carboxyethyl pyrrole-protein adducts could occur in photoreceptor cells before RPE phagocytosis of outer segment membrane or could occur within the lysosomal bodies in which RPE lipofuscin is stored, or both. The notion that oxidation processes are otherwise responsible for the formation of RPE lipofuscin, is not consistent with what is known regarding the composition of this material. For instance, the spectral properties of the blue-green emitting fluorescent products of lipid oxidation are substantially different (excitation maxima ~350, emission maxima ~ 435 nm) (Rein and Tappel, 1998) than spectra generated from RPE lipofuscin (Eldred and Katz, 1991; Eldred et al., 1982). Specifically, spectra obtained with intact RPE cells, RPE extracts (Eldred and Katz, 1991; Eldred et al., 1982), explants of adult human eyes (Delori et al., 1995) and suspensions of lipofuscin storage bodies (Boulton et al., 1990; Feeney-Burns and Eldred, 1983), have all demonstrated that RPE lipofuscin emits with an emission maximum of approximately 590–600 nm (yellow-orange) when excited by light in the ‘blue’ region of the spectrum. It has also been assumed that RPE lipofuscin consists of cross-linked oxidatively modified proteins (Brunk and Terman, 2002) derived from phagocytosed photoreceptor outer segments. However, Feeney-Burns and colleagues (Eldred and Katz, 1991; Eldred et al., 1982) and Boulton and colleagues (Boulton, 2009) have pointed out that the presence of photoreceptor proteins in preparations enriched in lipofuscin granules (lysosomal organelles) (Schutt et al., 2002; Warburton et al., 2005), is attributable to contamination with phagosomes. Moreover, a proteomic study of purified lipofuscin granules revealed that the amino acid content was only 2% (w/w) (Ng et al., 2008). It is also worth noting that the view that RPE lipofuscin accumulates because of inhibition of lysosomal enzymes, cannot be reconciled with the accumulation of this material in all healthy eyes even at young ages. Instead, it is likely that RPE lysosomal enzymes that would otherwise degrade the bisretinoid, do not recognize the unprecedented structures that constitute this material.

2. The composition of RPE lipofuscin

2.1. Known bisretinoids of retina

Considerable evidence has accumulated that, unlike the lipofuscin that accumulates in other non-dividing cells (Brunk and Terman, 2002), the lipofuscin pigments in RPE originate in photoreceptor cell outer segments (Katz et al., 1986) from random non-enzymatic reactions of retinaldehyde (Katz et al., 1987) (Fig. 1). Indeed, all of the constituents of RPE lipofuscin that have been isolated and characterized have been shown to form in this manner (Sparrow, 2007b; Sparrow et al., 2010a). The transfer from photoreceptor cell to RPE occurs with phagocytosis of shed outer segment membrane. Currently at least 25 bisretinoid pigments can be identified chromatographically and by mass spectrometry; these compounds can be grouped within 4 families: 1) A2E, the first RPE lipofuscin constituent to be described; 2) A2-glycerophosphoethanolamine (A2-GPE) a recently characterized pigment (Yamamoto et al., 2012); 3) A2-dihydropyridine-phosphatidylethanolamine (A2-DHP-PE); 4) all-*trans*-retinal dimer, all-*trans*-retinal dimer-phosphatidylethanolamine and all-*trans*-retinal dimer-ethanolamine ADD SAKAI (Ben-Shabat et al., 2002b; Fishkin et al., 2005; Kim et al., 2007a; Kim et al., 2007b; Liu et al., 2000; Parish et al., 1998; Wu et al., 2009; Yamamoto et al., 2012) (Fig. 1). Other chromatographic peaks having fluorescence and absorbance properties suggestive of bisretinoid, can be observed but the structures of the corresponding compounds are not yet known. The 25 peaks mentioned above include known isomers (e.g. *cis* isomers of A2E), some of the photooxidized forms of these bisretinoids and biosynthetic intermediates such as A2PE (Fig. 1, compound 7) and dihydropyridinium-A2PE (Fig. 1,

compound 5) (Section 3.2) (Fig. 1). Not included in this number, however, are bisretinoids differing in terms of the variety of fatty acid moieties that constitute the phospholipid-derived tails of some of these fluorophores (Section 3.2). The bisretinoids in RPE that retain the phospholipid moiety include all-*trans*-retinal dimer-PE and A2-DHP-PE (Fig. 1, compounds 6 and 10). A2E (Fig. 1, compound 8) on the other hand, does not carry fatty acids, since it is generated when its immediate precursor, the phosphatidylethanolamine-bisretinoid A2PE, undergoes phospholipase D-mediated enzymatic hydrolysis (Ben-Shabat et al., 2002b; Liu et al., 2000; Sparrow et al., 2008).

2.2. Topographic distribution

RPE lipofuscin, measured by recording autofluorescence, can be detected throughout the human retina, with the content increasing from the equator to the posterior pole except for a dip at the fovea (Weiter et al., 1986; Wing et al., 1978). Similarly, when human RPE/choroid is sampled by means of 4-mm trephine punches followed by chromatographic (430 nm detection) and mass spectrometric (*m/z* 592) analysis, A2E is found to accumulate centrally and in each of the 4 quadrants (Fig. 2). We have analyzed bisretinoid composition in human, mouse, rat and bovine eyes. In all cases, the same pigments are observed, although the relative levels of one bisretinoid to another can vary amongst these species.

2.3. Structural features of bisretinoids

Common to all of the known bisretinoids, is a ring structure in the core of the molecule. For instance, A2E and its isomers (Liu et al., 2000; Parish et al., 1998), A2-GPE (Yamamoto et al., 2012) and A2PE (Liu et al., 2000) are characterized by a central pyridinium ring that houses a quaternary amine nitrogen (Fig. 1, compounds 7,8,9). The nitrogen does not undergo deprotonation (Parish et al., 1998; Sparrow et al., 1999) and the positive charge on the pyridinium nitrogen is neutralized by a counter ion (probably chloride) making A2E a salt. While the double bonds along the side-arms of A2E are all in the *trans* (*E*) position, *Z*-isomers of A2E have double bonds at the C13/14 (isoA2E), C9/9'-10/10' and C11/11'-12/12' positions. A2-DHP-PE has a non-charged dihydropyridine ring at its core (Fig. 1, compound 10); this structure was confirmed by high performance liquid chromatography-electrospray ionization-tandem mass spectrometry with corroboration by Fourier transform infrared spectroscopy and modeling using density functional theory (Wu et al., 2009). On the other hand, the compound all-*trans*-retinal dimer contains a cyclohexadiene ring from which extend two polyene arms - 7 double-bond conjugations on the long arm and 4 on the short arm. All-*trans*-retinal dimer-E and all-*trans*-retinal dimer-PE are dimers of all-*trans*-retinal attached to PE via an imine function group (-C=N-) with a protonation state that is pH-dependent (Fishkin et al., 2005) (Fig. 1, compound 6).

3. Reactions in photoreceptor outer segments leading to bisretinoid formation

3.1. N-retinylidene-PE

All-*trans*-retinal that participates in bisretinoid biosynthesis is generated by photoisomerization of 11-*cis* retinal, following capture of a photon of light. In what is probably a mechanism for chaperoning all-*trans*-retinal, at least some of this aldehyde when released from photoactivated rhodopsin, reacts with phosphatidylethanolamine (PE) (1:1 ratio) in the disc membrane to form the adduct *N*-retinylidene-phosphatidylethanolamine (NRPE) (Fig. 1, compound 3) via an imine (Schiff base) linkage (Anderson and Maude, 1970; Liu et al., 2000; Poincelot et al., 1969; Sun et al., 1999; Weng et al., 1999). The sequestration of all-*trans*-retinal as NRPE may be an important mechanism limiting the toxicity of this reactive aldehyde.

NRPE is well known to be the ligand recognized by ABCA4, a member of the ABC (ATP-binding cassette) family of lipid transporters, that is thought to serve in the delivery of all-*trans*-retinal to cytosolic retinol dehydrogenases, a group of enzymes that reduce vitamin A aldehyde to the non-reactive alcohol form (Beharry et al., 2004; Molday et al., 2000; Molday and Molday, 1979; Papermaster et al., 1978; Sun et al., 1999; Sun and Nathans, 1997, 2001a, b; Weng et al., 1999). *ABCA4* is the gene responsible for recessive Stargardt disease (Allikmets et al., 1997). The Schiff base of NRPE can exist in either a protonated or unprotonated state but it is considered to be protonated when present in the acidic milieu of the disk lumen (Molday et al., 2009). The unprotonated form of NRPE binds to ABCA4 (Molday et al., 2009) and it is reported that in wild-type mice the unprotonated form predominates while *Abca4*$^{-/-}$ mice are associated with the protonated form (Weng et al., 1999). NRPE can readily undergo hydrolysis to release all-t*rans*-retinal; however, when NRPE reacts nonenzymatically with a second molecule of all-t*rans*-retinal, the irreversible formation of bisretinoid occurs (Fig. 1).

As shown in Figure 3, NRPE is a fluorescent molecule; at an excitation of 430 nm, the fluorescence efficiency of NRPE is 30% of A2E (A2E fluorescence/absorbance, 0.18; NRPE fluorescence/absorbance, 0.05). Analysis of eye extracts obtained from *Abca4*$^{-/-}$ mice reveals that NRPE can form by reaction with diacyl-PE comprised of various fatty acids and degrees of saturation, for instance 22:6 (docosahexaenoic acid, DHA) and 18:0 (stearic acid) (Fig. 3). Not surprisingly, DHA is a predominant constituent of these adducts due to its abundance in outer segment membrane (Fliesler and Anderson, 1983). In addition, however, we found that NRPE can form as a Schiff base conjugate between all-*trans*-retinal and both ether-PE (e.g. C22:5 and 18:0, Fig. 3) and PE-based plasmalogens (e.g. C22:5 and 18:1, Fig. 2); ether-PE and ethanolamine plasmalogens are both lipid constituents of outer segments (Anderson and Maude, 1970). PE may not be the only amine-bearing molecule that interacts with all-*trans*-retinal however, since we have also observed that pairs of all-*trans*-retinal (A2) can covalently attach to the lysine residues of rhodopsin (Fishkin et al., 2003). As yet, however, we have not detected A2-peptides in RPE lipofuscin.

3.2. Formation of A2PE and A2E

The formation of NRPE from all-*trans*-retinal and PE is the first step in the multi-step process by which at least some retinal bisretinoids are generated (Fig. 1). For instance, A2E forms when NRPE reacts non-enzymatically with a second molecule of all-t*rans*-retinal and the biosynthetic pathway continues with the generation of a dihydropyridinium molecule (dihydropyridinium-A2PE) (Fig. 1, compound 5). Dihydropyridinium-A2PE subsequently undergoes autooxidation to eliminate two hydrogens (Ben-Shabat et al., 2002b; Kim et al., 2007a; Liu et al., 2000; Parish et al., 1998) and yield A2PE (Fig. 1, compound 7), a positively charged phosphatidyl-pyridinium bisretinoid. Phospholipase D-mediated cleavage of A2PE generates A2E and establishes A2PE as the immediate precursor of A2E (Ben-Shabat et al., 2002b; Liu et al., 2000). This hydrolytic activity is present in lysosomal fractions of RPE (Sparrow et al., 2008).

The formation of bisretinoid in photoreceptor outer segments (POS) can be observed by analyzing POS isolated from bovine eyes. As presented in Fig 4, one of these, the pigment A2PE, forms in outer segments as the immediate precursor of A2E. A2PE is not a single molecule but a complex mixture consisting of fatty acids of varying lengths and degrees of unsaturation, for instance 22:6 (docosahexaenoic, DHA) and 18:0 (stearic acid) (Fig. 4). Incubation of bovine outer segments with all-*trans*-retinal mimics bisretinoid formation *in vivo* and by intensifying the detection of these A2PE species (Fig. 4C), confirms their formation by all-t*rans*-retinal reactivity.

In a series of experiments, we varied the ratio of all-*trans*-retinal to PE in synthetic mixtures to determine how these two precursors might affect A2PE formation (Fig. 5). We found that the yield of A2PE increased when the ratio of equivalents of all-t*rans*-retinal to PE (egg-PE as starting material) was increased from 1:2 to 2:2 and then 4:2 equivalents (Fig. 5 A). No further increase was observed at 8 equivalents of all-t*rans*-retinal (8:2 ratio) indicating that A2-adduct formation saturated at an equivalent ratio of 4:2 (all-t*rans*-retinal to PE). On the other hand, increasing the concentration of PE from an equivalents ratio of 4:1 through 4:8 (all*trans*-retinal to PE) resulted in a steady increase in A2PE synthesis product yield (Fig. 5 B). These findings indicate that the concentration of PE has a pronounced effect on the rate of A2PE synthesis. In particular, the first step in the synthetic pathway, the formation of NRPE, is expected to be the most facile reaction in the pathway. Interestingly, increasing PE in the reaction mixture also promoted all-*trans*-retinal dimer formation (Fig. 5 C), an observation supporting our previous suggestion that PE is an early participant in reactions leading to all-*trans*-retinal dimer synthesis (Fishkin et al., 2005). These findings are significant since in the *Abca4*$^{-/-}$ mouse, a model in which bisretinoid forms in abundance, the level of PE in the outer segment membrane is reported to be increased (Weng et al., 1999). Pepperberg and colleagues have suggested that the higher level of PE in *Abca4*$^{-/-}$ mice may facilitate sequestering of all-*trans*-retinal as NRPE, thereby accelerating recovery of the rod photoresponse after a 30–40% bleach (Pawar et al., 2008).

Since 22:6n-3 (DHA) is an abundant unsaturated fatty acid in photoreceptor cell outer segments and is acquired through dietary intake, we also compared the yield of A2PE when 22:6n-3-containing PE was precursor versus egg-PE (a mixture of fatty acid moieties) (Fig. 5D). A2PE production was greater with egg-PE. On the other hand, if free DHA was added to the egg-PE/all-trans-retinal reaction mixture, the yield of A2PE was increased (Fig. 5 E). DHA content has been shown to have several effects on retina (Tanito et al., 2009) including susceptibility to light damage, but whether modulation of bisretinoid formation is involved, it is not known. We also found that under deprotonating conditions associated with the addition of base (triethylamine) to the reactants, the generation of A2PE was increased (Fig. 5 F).

3.3. Formation of A2-DHP-PE

While elimination of two hydrogens from dihydro-pyridinium-A2PE leads to the formation of A2PE in the A2E synthetic path, hydrogen transfer and one hydrogen elimination yields the uncharged and stable dihydropyridine compound, A2-DHP-PE (A2-dihydropyridine-phosphatidylethanolamine) (Wu et al., 2009) (Fig. 1, compound 10). Conditions that favor A2-DHP-PE formation rather than A2PE, are not yet known. A2-DHP-PE is amongst the bisretinoids detected in human, mouse and bovine RPE and as is the case for other bisretinoids of RPE lipofuscin, it accumulates with age. In the human eye, the ratio of A2E to A2-DHP-PE is approximately 1:1 (Wu et al., 2009).

3.4. Formation of all-trans-retinal dimer and conjugates

A dimer of all-*trans*-retinal (all-*trans*-retinal dimer) is produced when two molecules of all-*trans*-retinal condense; this aldehyde-bearing dimer can then proceed to react with the amine of PE to form a conjugate with PE (all-*trans*-retinal dimer-PE) via a Schiff base linkage that is protonated (Fishkin et al., 2005; Kim et al., 2007b) (Fig. 1, compound 4 and 6). We have proposed a mechanism by which all-*trans*-retinal dimer may form after reaction of NRPE with a second molecule of all-*trans*-retinal (Fishkin et al., 2005). All-*trans*-retinal dimer-PE is particularly abundant in eyes harvested from *Abca4* null mutant (*Abca4*$^{-/-}$) mice (Kim et al., 2007b) (Section 7.1).

3.5. Formation of A2-GPE

The most recent RPE bisretinoid to be identified, exists as a conjugate of two all-*trans*-retinal and glycerophosphoethanolamine (GPE) (Fig. 1, compound 9) (Yamamoto et al., 2012). A2-GPE was found to accumulate with age in human and mouse eyes and was more abundant in *Abca4*$^{-/-}$ mice, a model of recessive Stargardt disease (Section 7.1). We have suggested that A2-GPE may form by direct bisretinoid adduction on GPE or it may be generated secondary to A2PE catabolism. Direct bisretinoid adduct formation on GPE would indicate that in addition to A2-adducts on PE, glycerophosphoethanolamine is available for reaction.

4. Absorbance and emission spectra

4.1. Structural features underlying bisretinoid absorbance and fluorescence emission

All of the isolated bisretinoids of RPE lipofuscin exhibit a central 6-membered ring from which extends dual polyene arms terminating in β-ionine rings (Fig. 1). Each of the arms constitutes a separate system of double bond conjugations, and as such, each serves as a chromophore, one arm absorbing in the ultraviolet and the other in the visible region of the spectrum. Absorbances in the visible spectrum are significant since these wavelengths reach the retina.

The wavelengths at which bisretinoids absorb are determined by the length of the systems of alternating double and single bonds, including the double bonds in the β-ionone and central rings, if continuous with the chain conjugations. For instance, A2E has an absorbance maximum in the visible spectrum at ~ 440 nm that can be assigned to the long arm and a shorter wavelength absorbance at ~ 340 nm that is generated within the short arm. The additional red-shift to 510 nm absorbance exhibited by all-*trans*-retinal dimer-PE and all-*trans*-retinal dimer-E, occurs due to protonation of the Schiff base nitrogen (Fishkin et al., 2005; Kim et al., 2007b). Accordingly, the bisretinoid pigments exhibit differences in their absorbance maxima: A2E-A2E/isoA2E, λ_{max} ~ 340, 440 nm; all-*trans*-retinal dimer, λ_{max} ~ 290, 432 nm; all-*trans*-retinal dimer-E/all-*trans*-retinal dimer-PE, λ_{max} ~ 290, 510 nm; and A2-DHPPE, λ_{max} ~ 333, 490 nm. As noted above, some of the bisretinoids retain a phospholipid moiety, but this portion of the molecule does not make a contribution to absorbance at wavelengths greater than 250 nm.

4.2. Comparing the fluorescence emission spectra of human lipofuscin and A2E

Given the varying absorbances presented above, it is not surprising that fluorescence emission spectra can be recorded from RPE lipofuscin over a range of excitation wavelengths. As shown in Figure 6 A, if the fluorescence emission spectrum obtained from the lipofuscin in the human RPE monolayer is compared with the spectrum obtained from cells containing A2E only, the spectra are revealed to be similar in shape with 488 nm excitation. The emission maxima for both are approximately 590 nm, the same maximum originally reported by Eldred for whole RPE lipofuscin (Eldred and Katz, 1991; Eldred et al., 1982). The spectral width (at half-maximal intensity) for A2E and whole lipofuscin are also similar (133 nm and 136 nm for A2E and human lipofuscin, respectively) in this recording. A difference is evident however with 561 nm excitation in that a fluorescence spectrum can be generated from whole human lipofuscin but A2E exhibited little fluorescence at the longer wavelength excitation (561 nm). It is worth noting that at 561 nm excitation the peak emission recorded for human lipofuscin is red-shifted to 620 nm and the spectral width is narrower (96 nm). These features are indicative of a lipofuscin composed of a mixture of pigments with different, but overlapping, subsets of fluorophores being excited as the excitation wavelength is changed.

4.3. Fluorescence emission spectra of lipofuscin in RPE of Abca4 null mutant mice

In *Abca4*$^{-/-}$ mice, the accumulation of bisretinoid lipofuscin is accentuated (Kim et al., 2004; Weng et al., 1999). The emission spectrum of RPE lipofuscin measured using histological sections of *Abca4*$^{-/-}$ mice can also be obtained using a range of excitation wavelengths (Fig 6B). The fluorescence emission intensity increases with age from 2 to 8 months in the mutant mice.

4.4. Changes in fluorescence emission with irradiation of bisretinoid

When excited at 430 nm, A2E and isoA2E have relatively broad emission spectra with maxima at ~ 600 nm (Sparrow et al., 1999) (Fig 6C), an orange fluorescence. After irradiation (430 nm) for 2 minutes however, A2E fluorescence intensity (with 440 nm excitation) decreases and exhibits a blue-shifted emission maximum (Fig 6C). The spectral width, measured at half-maximal intensity, also increases, the extension of the spectral profile occurring toward shorter wavelengths. The latter change reflects an increasingly complex mixture due to photooxidation of A2E (Section 5).

5. Photodegradation of RPE bisretinoids

Efforts to understand the damaging effects of RPE lipofuscin have lead to the study of lipofuscin photoreactivity. Early on, photo-dependent uptake of oxygen was detected in both suspensions of RPE cells and in lipofuscin granules (Pawlak et al., 2002; Rozanowska et al., 1995; Rozanowska et al., 2002; Rozanowska et al., 2004) and the rate of oxygen uptake was shown to increase with age (Rozanowska et al., 1995; Rozanowska et al., 2002; Rozanowska et al., 2004). Production of singlet oxygen and superoxide anion was also demonstrated. (Gaillard et al., 1995; Reszka et al., 1995; Rozanowska et al., 1995; Rozanowska et al., 1998). Luminescence studies based on the detection of a characteristic phosphorescence at 1270 nm, and by measuring singlet-oxygen-mediated production of cholesterol hydroperoxides, demonstrated that photoexcitation of A2E leads to singlet oxygen production (Ben-Shabat et al., 2002a; Pawlak et al., 2003). Measurements of the quantum yield of singlet oxygen production by A2E have provided widely varying results (Kanofsky et al., 2003; Lamb et al., 2001), in large part because the conjugated double bond structure serves to quench the singlet oxygen as generated (Ben-Shabat et al., 2002a; Roberts et al., 2002). Singlet oxygen and superoxide anion production and singlet oxygen quenching are even more pronounced for unconjugated all-*trans*-retinal dimer than for A2E (Kim et al., 2007b) and the photooxidation of these bisretinoids (Fig. 7) leads to the formation of epoxides, furanoid moieties and endoperoxides (Jang et al., 2005; Kim et al., 2007b).

Photo-exposure of A2E-containing RPE can lead to cell damage and death (Schutt et al., 2000; Sparrow et al., 2000). Given the short life-time of singlet oxygen and the realization that singlet oxygen is quenched by the polyene chains of the bisretinoids (Ben-Shabat et al., 2002a; Roberts et al., 2002), it is unlikely that cellular damage occurs as a direct consequence of singlet oxygen generation. Instead, the deleterious effects are mediated by the photooxidation (Ben-Shabat et al., 2002a; Sparrow et al., 2002), and photodegradation products of bisretinoid that result from singlet oxygen addition at the carbon-carbon double bonds (Fig. 7). We demonstrated the reactivity of these photoproducts by assaying the activity of cellular GAPDH (glyceraldehyde 3-phosphate dehydrogenase), a well known redox sensitive thiol-containing enzyme that is subject to oxidation related inhibition (Ferri et al., 1978; Lee et al., 2005). We measured the cellular activity of GAPDH using an assay whereby NADH generated from GAPDH activity converts the chromogenic substrate 2-(4-iodophenyl)-3-(4-nitrophenyl)-5-phenyl tetrazolium to formazan. In ARPE-19 cells that had accumulated A2E and were irradiated at 430 nm to induce photooxidation/photofragmentation of A2E, GADPH activity was decreased by approximately 50% (Fig. 8).

Utilizing liquid chromatography (LC) coupled to electrospray ionization mass spectrometry (ESI-MS) together with tandem mass spectrometry (MS/MS), we have shown that A2E (Wu et al., 2010b) and all-*trans*-retinal dimer (Fig. 7) undergo photooxidation-induced degradation at sites of singlet molecular oxygen addition thereby releasing aldehyde-bearing cleavage products (Wu et al., 2010b) (Fig. 7). Importantly, the photodegradation products of A2E and all-*trans*-retinal dimer include methylglyoxal and glyoxal, small, reactive oxo-aldehydes with the capacity to form advanced glycation end (AGE) products (Fig. 9). In chronic diseases such as diabetes and atherosclerosis, methylglyoxal and glyoxal form as intermediates in the non-enzymatic glycation and oxidation reactions that modify proteins by AGEs. AGE-modified proteins are also detected in deposits (drusen) that accumulate below RPE cells *in vivo*; drusen are a major risk factor for AMD progression (Farboud et al., 1999; Glenn et al., 2007; Handa et al., 1999; Ishibashi et al., 1998). Bisretinoid photocleavage upon exposure to wavelengths of light that reach the retina, is a previously unknown source of methylglyoxal and glyoxal and likely serves as the origin of the dicarbonyls that play a role in drusen formation. These findings also indicate a link between RPE lipofuscin photooxidation and drusen formation. The photolysis of bisretinoid molecules following photooxidation explains the observation that photooxidized forms of A2E do not accumulate with age (Grey et al., 2011).

It is important to note that the photooxidative processes described above occur *in vivo*. Specifically, mono- and bis-peroxy-A2E, mono- and bis-furano-A2E, mono- and bis-peroxy-all-*trans*-retinal dimer and mono-and bis-furano-all-*trans*-retinal dimer are detected in extracts from human and mouse eyes (Jang et al., 2005; Kim et al., 2007b).

6. Retinal bisretinoids and fundus autofluorescence

The retina, even under healthy conditions, exhibits a natural autofluorescence (fundus autofluorescence) that can be imaged non-invasively for clinical examination and study. The spectral characteristics and age-dependent intensification of this autofluorescence are consistent with the source being the bisretinoids of retina (Delori et al., 2011; Delori et al., 2007; Sparrow, 2007a; Sparrow et al., 2010c). Studies of the tissue distribution have localized the autofluorescence primarily to the RPE monolayer in the healthy eye.

Although RPE bisretinoids exhibit a variety of excitation maxima (Section 4.1), they all emit a fluorescence that is centered approximately around 600 nm. This emission is similar to the maximum emission of fundus autofluorescence (Delori et al., 2007). As is also the case for fundus autofluorescence (Delori et al., 2007) and RPE lipofuscin (Sparrow et al., 2010b), individual retinal bisretinoids exhibit a small but characteristic red-shift with increasing excitation wavelength (Fig. 5).

Abnormal patterns of autofluorescence are a feature of some retinal disorders. In terms of actual changes in bisretinoid levels, regions of reduced or absent fundus autofluorescence can reflect RPE cell atrophy or death (Holz et al., 2001; Robson et al., 2008b). Parafoveal rings of intense autofluorescence are often observed in patients with retinitis pigmentosa (Robson et al., 2008b) while outward-expanding autofluorescent rings can be visualized in *ABCA4*-related retinal disease (Michaelides, 2009; Robson et al., 2008a; Robson et al., 2008b). Under these conditions, aberrant autofluorescence from excessive production of bisretinoid by impaired photoreceptor cells may serve as an additional source of fundus autofluorescence (Sparrow et al., 2010c). Alterations in fundus autofluorescence that do not reflect changes in bisretinoid level could be accounted for by RPE cell migration and clumping.

Efforts are currently ongoing to extend the resolution of fundus AF imaging through the incorporation of adaptive optics to scanning laser ophthalmoscopy. Surprisingly, preclinical

studies in non-human primates have revealed that the use of light levels (≥247 J/cm^2) below light safety standards (American National Standards Institute, 2007) results in photobleaching of RPE lipofuscin along with notable RPE cell damage (Hunter et al., 2011; Morgan et al., 2009). Since the photobleaching observed reflects bisretinoid photooxidation and degradation (Hunter et al., 2011), these observations call attention to the role of these photoreactive pigments in light damage and indicate that the RPE may be more susceptible to light damage than previously recognized. Also unanswered are questions concerning the involvement of RPE versus photoreceptor cells in photochemical damage. Furthermore, since at considerably lower light levels (≥5 J/cm^2) photobleaching can also occur in the absence of RPE cell damage, it is clear that the processes of photooxidation and photodegradation can be ongoing without acute cell death.

Compounds other than those present in RPE lipofuscin have been suggested as the source of fundus autofluorescence. For instance, cellular flavoproteins (Field et al., 2008) in the oxidized state absorb at 460 nm and emit at 530 nm (Kindzewlskii and Petty, 2004). Flavoproteins participate in mitochondrial electron transport and their fluorescence has been used to monitor the metabolic status of cells, the amount of flavoprotein autofluorescence being inversely related to mitochondrial activity. However, it should be kept in mind that flavoproteins are not specific to RPE and thus would emit from any or all cells of retina, a pattern that is not typical of fundus autofluorescence.

There has also been considerable interest in whether drusen are the source of fundus autofluorescence. Although autofluorescence levels at sites of drusen, are not appreciably different from background (Holz et al., 2001; Lois et al., 2002; von Ruckmann et al., 1997), in histological sections of human macula viewed under a fluorescence microscope, some sub-RPE deposits have a blue-green fluorescence; the latter reflects a shift toward shorter wavelengths relative to RPE lipofuscin (Marmorstein et al., 2002). Detailed analysis of the topography of autofluorescence over drusen has shown that for both hard and soft drusen (60 – 175 mm in size), there is a distinct annulus of hyperfluorescence over the outer edge of the druse and lower autofluorescence over the center. This pattern is thought to reflect drusen-associated displacement and thinning of RPE cells (Delori et al., 2000).

7. Learning from human disease and animal models

7.1. ABCA4-deficiency

As discussed in Section 3.2, excessive bisretinoid lipofuscin accumulation is a feature of diseases caused by *ABCA4* gene mutations in humans. Bisretinoid pigments likely also account for the lipofuscin-like autofluorescence that can be visualized in the photoreceptor cell membrane in some forms of ABCA4-linked disease (Birnbach et al., 1994; Bunt-Milam et al., 1983; Szamier and Berson, 1977). Mutations in the *ABCA4* gene are responsible for recessive Stargardt macular degeneration, recessive cone-rod dystrophy and recessive retinitis pigmentosa (Cremers et al., 1998). While the severity of the disease phenotype is suggested to be inversely related to the level of residual protein activity (Shroyer et al., 1999), it is also noted that some mutations, particularly those in the C-terminus, are associated with misfolded protein that is retained in the endoplasmic reticulum, so there is the possibility that simple loss of function does not always account for disease severity (Cideciyan et al., 2009; Zhong et al., 2009). The abundant RPE lipofuscin observed in ABCA4-related disease in humans, is recapitulated in the *Abca4* null mutant mouse (Kim et al., 2004; Weng et al., 1999). Studies in the *Abca4*$^{-/-}$ mice have also revealed an association between excessive RPE lipofuscin accumulation and photoreceptor cell death. In particular, analysis of outer nuclear layer thickness, as an indicator of photoreceptor cell survival has revealed that albino *Abca4*$^{-/-}$ mice display progressive photoreceptor cell loss that is clearly detectable at 8 months of age and that has worsened by 12 and 13 months of age (Wu et al.,

2010a). Photoreceptor cell degeneration was independently observed in 11-month-old albino *Abca4*$^{-/-}$ mice (Radu et al., 2008). Delivery of the human ABCA4 gene via lentiviral (Kong et al., 2008), adeno-associated virus (Allocca et al., 2008) vector to the subretinal space of *Abca4*$^{-/-}$ mice, reduces disease-associated A2E accumulation.

7.2. Light exposure and vitamin A supplementation

Since the bisretinoid lipofuscin fluorophores form from random inadvertent reactions between all-*trans*-retinal and amine-containing compounds, and since the production of all-*trans*-retinal is light-dependent, it is not surprising to find that exposure to light influences the formation of these vitamin A-related pigments. Specifically, it has been shown that bright light augments the formation of A2PE in photoreceptor outer segments (Ben-Shabat et al., 2002b) while dark rearing of mice depresses the deposition of A2E in the RPE (Mata et al., 2000). Mice, both wild-type and *Abca4* null mutant, that are given a vitamin A supplemented diet also exhibit increased levels of A2E as compared to mice fed a control diet (Radu et al., 2008). The investigators suggested that this increase was likely attributable to a faster rate of visual chromophore regeneration and a concomitant increase in the rate of 11-*cis*-retinal photoisomerization to all-*trans*-retinal, yielding heightened bisretinoid formation.

7.3. Modulation of retinal bisretinoid formation by RPE65

In contrast to the abundant RPE lipofuscin formation associated with *ABCA4* deficiency, knock-out of the RPE65 gene in mice leads to an absence or pronounced decrease in RPE lipofuscin (Katz and Redmond, 2001). Similarly, in Lebers congenital amaurosis due to *RPE65* mutations, there is an absence or pronounced decrease in RPE lipofuscin as detected by fundus autofluorescence imaging (Lorenz et al., 2004). Lebers congenital amaurosis is a severe form of retinal degeneration with onset in children. The function of RPE65 In the visual cycle, is to serve in the conversion of all-*trans*-retinyl esters to 11-*cis*-retinol (Jin et al., 2005; Moiseyev et al., 2005; Redmond et al., 2005). The absence of RPE65 results in a failure to produce the 11-*cis*-retinal chromophore, so all-*trans*-retinal that is the essential precursor for bisretinoid formation, is not generated and bisretinoid lipofuscin does not form. An amino acid change (Leu450Met) that reduces levels of Rpe65 in mouse RPE, (Lyubarsky et al., 2005; Nusinowitz et al., 2003) also lowers A2E formation (Kim et al., 2004), as can small molecule inhibitors that target RPE65 function (Golczak et al., 2005; Maiti et al., 2006).

7.4. Mutations in retinol dehydrogenase (RDH)

Other visual cycle genes also impact RPE lipofuscin formation. For instance, mutant mice deficient in enzymes that reduce all-*trans*-retinal to the alcohol form (e.g. retinol dehydrogenase-8, Rdh8; Rdh12) exhibit pronounced increases in A2E as compared to wild-type mice (Chrispell et al., 2009; Maeda et al., 2008). This abnormality occurs because the photoreceptor cell is deprived of avenues for inactivating all-*trans*-retinal. Mutations in human RDH12 gene are responsible for a subset of cases of Leber Congenital Amaurosis (Janecke et al., 2004).

7.5. ELOVL4-related macular dystrophy

Mutations in *ELOVL4* (elongation of very long chain fatty acids protein 4), the gene responsible for early-onset dominant Stargardt-like macular degeneration, are also reported to result in increased levels of RPE lipofuscin. Frame-shift mutations in ELOVL4 result in premature termination of the protein, aggregate-formation with the wild-type protein and mislocalization of the protein (Grayson and Molday, 2005; Karan et al., 2005b; Vasireddy et al., 2005; Zhang et al., 2001). Transgenic mice expressing the mutant protein exhibit modest

elevations in RPE lipofuscin, measured as A2E (Karan et al., 2005a; Vasireddy et al., 2009; Vasireddy et al., 2005). ELOVL4 is required for the synthesis of C28 and C30 saturated fatty acids, and the synthesis of C28-C38 very long chain polyunsaturated fatty acids, the latter being abundant in retina (Agbaga et al., 2008). Nevertheless, the link to enhanced bisretinoid formation is not understood.

7.6. Senescence-accelerated mice

Bisretinoids accumulate in RPE cells with age because the cell is not able to metabolize this material. However, cellular aging, per se, is not the cause of RPE bisretinoid formation. For instance, lipofuscin can be detected in human RPE during the first decade of life (Wing et al., 1978) and can also be measured in young mice (Kim et al., 2007b; Yamamoto et al., 2012). Nevertheless, to evaluate whether aging itself might aggravate bisretinoid formation we examined mice that exhibit accelerated senescence (senescence accelerated mouse-prone, SAMP) (Fig. 10). These mice exhibit early retina changes such as Bruch's membrane thickening and loss of photoreceptor cells (Majji et al., 2000; Nomura et al., 2004). In HPLC analysis of A2E/isoA2E levels in the mouse eyes, we observed an early increase in the bisretinoid that was demonstrable by 4 months of age and then declined. By measuring outer nuclear layer (ONL) thickness in retinal sections, we observed an appreciable decrease in the ONL at 6 months of age relative to control mice (senescence accelerated mouse-resistant; SAMR).

7.7. Age-related macular degeneration

Dysregulation of complement activation is considered to underlie the association between susceptibility to age-related macular degeneration and certain genetic variants in complement factors (Edwards et al., 2005; Hageman et al., 2005; Haines et al., 2005; Klein et al., 2005). In terms of initiators of complement activation, we have shown using differentiated cultures of human fetal RPE (Zhou et al., 2009) and ARPE-19 cells (Zhou et al., 2006) that photooxidation products of A2E and all-*trans*-retinal dimer can activate complement while depletion of factor B reduces complement activation as does an inhibitor of complement 3 (C3) (Zhou et al., 2006; Zhou et al., 2009). The addition of C-reactive protein in these assays also suppresses complement activation. In support of these findings, vigorous complement activation has been observed in the *Abca4*$^{-/-}$ mouse, a model defined by pronounced RPE bisretinoid (Radu et al., 2011). While AMD has onset in the elder years it likely develops for several years before diagnosis. Complement activation triggered by photooxidation products of RPE bisretinoid lipofuscin could begin early in life and generate low-grade inflammatory processes that gradually, along with other factors, predispose the macula to disease.

7.8. Conditions of oxidative stress

Ribozyme-mediated knock-down of MnSOD2 in the mouse is associated with an increase in A2E when measured by high performance liquid chromatography (Justilien et al., 2007). The antioxidant enzyme MnSOD2 is encoded by the nuclear gene SOD2, the protein is localized to mitochondria and the enzyme catalyzes the conversion of superoxide anion (generated by aerobic respiration) to hydrogen peroxide. The mechanism by which A2E formation is increased in the presence of a deficiency in SOD2 is not clear. The formation of A2E involves an automatic oxidation step whereby two hydrogens are eliminated from dihydropyrdinium-A2PE (Parish et al., 1998). We have shown that deoxygenation under argon allows dihydropyridinium-A2PE to collect and A2E formation is reduced (Kim et al., 2007a). However, diatomic ground state oxygen would readily accept these hydrogens and one would not expect the A2E synthetic pathway to fluctuate with changing levels of reactive forms of oxygen. Thus one has also to consider other mechanisms. It is conceivable that in the setting of SOD2 deficiency, compensatory mechanisms come into play. For

instance, the reduced form of glutathione (GSH) can detoxify superoxide anion radical by reacting with it (Dickinson and Forman, 2002). Oxidized glutathione (GSSG) is subsequently converted back to GSH in a redox cycle involving glutathione reductase and the electron acceptor NADPH (nicotinamide adenine dinucleotide). Perhaps depletion of NADPH in this way, could interfere with NADPH-dependent reduction of all-*trans*-retinal to retinol, the availability of the former allowing for increased A2E formation.

8. Conclusions and Future Directions

It is generally considered that in juvenile onset recessive Stargardt disease, the overproduction of bisretinoid and its accumulation as lipofuscin in RPE cells, are the causes of RPE atrophy and photoreceptor cell degeneration. Corroborating evidence of this causality could come from the analysis of clinical outcomes achieved with therapeutic strategies aimed at reducing bisretinoid formation by limiting the visual cycle. RPE cell density in the human eye is also reduced with age (Del Priore et al., 2002), although a relationship between this loss and the amassing of bisretinoid has not been shown. Healthy retinas of similar age vary substantially in terms of levels of bisretinoid levels (Delori et al., 2001; Delori et al., 2011), but the factors responsible for these differences have not been elucidated. Also unknown is the pathway from a mutation in *ELOVL4* to elevated bisretinoid accumulation (Section 7.5).

RPE lipofuscin consists of a mixture of bisretinoids, only some of which have been characterized. Missing from our understanding are conditions that favor the formation of one bisretinoid over another. Efforts to clarify the composition of RPE lipofuscin are important since these compounds are targets of gene-based and drug therapies that aim to alleviate *ABCA4*-related retinal disease. Importantly, the various bisretinoid pigments have different properties (Sparrow et al., 2010a). For instance, while whole RPE lipofuscin exhibits fluorescence when excited with 561 nm light (Fig. 6A), A2E does not. Consequently, at the wavelength (568 nm) used to record fundus autofluorescence by adaptive optics/ scanning laser ophthalmoscopy (Section 6), there is unlikely to be appreciable A2E excitation. Thus the RPE damaged elicited by 568 nm exposure must involved photoreactive processes involving bisretinoids other than A2E.

We have provided evidence that bisretinoid photodegradation can serve as a source of the dicarbonyl molecules responsible for AGE-modification of protein, such as is observed in drusen (Wu et al., 2010b). It is clear that bisretinoid photooxidation is ongoing in *in vivo* retina since the photooxidized forms of A2E and all-trans-retinal dimer are detected in human and mouse RPE (Jang et al., 2005; Kim et al., 2007b). As might be expected, however, these photooxidized species do not accumulate with age (Grey et al., 2011), since the oxidation lead to bisretinoid fragmentation. The processes of photooxidation and photodegradation mechanisms such as these may point to links amongst factors posited as being associated with AMD including oxidative processes, complement dysregulation, light exposure and drusen formation.

Given the wide-spread use of fundus autofluorescence imaging in the diagnosis of retinal disease, continued efforts to better understand RPE lipofuscin will also inform interpretations of these images (Sparrow et al., 2010b; Sparrow et al., 2010c). Progress has been made in the implementation of methods to quantify fundus autofluorescence so as to correlate levels of fundus autofluorescence with disease severity (Delori et al., 2011). The assumption is that AF intensity is a measure of the amount of lipofuscin in the RPE monolayer and thus can be used to gauge the health of the cells. There may be exceptions to this interpretation however, since in the case of some patterns of AF, high intensity fluorescence may be attributable to anomalous but greatly elevated lipofuscin formation in

impaired photoreceptor cells (Sparrow et al., 2010c). Moreover, given the evidence for photodegradation of bisretinoid, measurements of AF are unlikely to be indicative of amounts of bisretinoid accumulated over a lifetime of accumulation and therefore are not indicative of the total lipofuscin burden. Indeed the amount lost and therefore not measurable may be more informative of RPE cell status.

Abbreviations

ABCA4	ATP-binding cassette, sub-family A, member 4
DHA	docosahexaenoic acid
ESI-MS	electrospray ionization mass spectrometry
GAPDH	glyceraldehyde 3-phosphate dehydrogenase
GSH	glutathione
mSOD2	mitochondrial superoxide dismutase-2
NRPE	*N*-retinylidene-phosphatidylethanolamine
PE	phosphatidylethanolamine
RDH	retinol dehydrogenase
RPE	retinal pigment epithelium

Acknowledgments

This work was supported by National Institutes of Health grants EY12951 (JRS) and P30EY019007 and a grant from Research to Prevent Blindness to the Department of Ophthalmology. The Carl Marshall Reeves and Mildred Almen Reeves Foundation provided funds for equipment. EGR was supported by an Endeavour Australia Research Fellowship and Lucy Falkiner Fellowship. Drs. Yalin Wu, Emiko Yanase, Chul Young Kim and Kee Dong Yoon are acknowledged for contributions.

References

Agbaga MP, Brush RS, Mandal MN, Henry K, Elliott MH, Anderson RE. Role of Stargardt-3 macular dystrophy protein (ELOVL4) in the biosynthesis of very long chain fatty acids. Proc Natl Acad Sci U S A. 2008; 105:12843–12848. [PubMed: 18728184]

Allikmets R, Singh N, Sun H, Shroyer NF, Hutchinson A, Chidambaram A, Gerrard B, Baird L, Stauffer D, Peiffer A, Rattner A, Smallwood P, Li Y, Anderson KL, Lewis RA, Nathans J, Leppert M, Dean M, Lupski JR. A photoreceptor cell-specific ATP-binding transporter gene (ABCR) is mutated in recessive Stargardt macular dystrophy. Nat Genet. 1997; 15:236–246. [PubMed: 9054934]

Allocca M, Doria M, Petrillo M, Colella P, Garcia-Hoyos M, Gibbs D, Kim SR, Maguire AM, Rex TS, Di Vicino U, Cutillo L, Sparrow JR, Williams DS, Bennett J, Auricchio A. Serotype-dependent packaging of large genes in adeno-associated viral vectors results in effective gene delivery in mice. J Clin Invest. 2008; 118:1955–1964. [PubMed: 18414684]

Anderson RE, Maude MB. Phospholipids of bovine outer segments. Biochemistry. 1970; 9:3624–3628. [PubMed: 5509846]

Beharry S, Zhong M, Molday RS. N-retinylidene-phosphatidylethanolamine is the preferred retinoid substrate for the photoreceptor-specific ABC transporter ABCA4 (ABCR). J Biol Chem. 2004; 279:53972–53979. [PubMed: 15471866]

Ben-Shabat S, Itagaki Y, Jockusch S, Sparrow JR, Turro NJ, Nakanishi K. Formation of a nona-oxirane from A2E, a lipofuscin fluorophore related to macular degeneration, and evidence of singlet oxygen involvement. Angew Chem Int Ed. 2002a; 41:814–817.

Ben-Shabat S, Parish CA, Vollmer HR, Itagaki Y, Fishkin N, Nakanishi K, Sparrow JR. Biosynthetic studies of A2E, a major fluorophore of RPE lipofuscin. J Biol Chem. 2002b; 277:7183–7190. [PubMed: 11756445]

Birnbach CD, Jarvelainen M, Possin DE, Milam AH. Histopathology and immunocytochemistry of the neurosensory retina in fundus flavimaculatus. Ophthalmology. 1994; 101:1211–1219. [PubMed: 8035984]

Boulton M, Docchio F, Dayhaw-Barker P, Ramponi R, Cubeddu R. Age-related changes in the morphology, absorption and fluorescence of melanosomes and lipofuscin granules of the retinal pigment epithelium. Vision Res. 1990; 30:1291–1303. [PubMed: 2219746]

Boulton, ME. Lipofuscin of the retinal pigment epithelium. In: Lois, N.; Forrester, JV., editors. Fundus Autofluorescence. Philadelphia: Wolters Klumer/Lippincott Williams and Wilkins; 2009. p. 14-26.

Brunk UT, Terman A. Lipofuscin: mechanisms of age-related accumulation and influence on cell function. Free Rad Biol Med. 2002; 33:611–619. [PubMed: 12208347]

Bunt-Milam AH, Kalina RE, Pagon RA. Clinical-ultrastructural study of a retinal dystrophy. Invest Ophthalmol Vis Sci. 1983; 24:458–469. [PubMed: 6682096]

Chio KS, Reiss U, Fletcher B, Tappel AL. Peroxidation of subcellular organelles: formation of lipofuscin-like fluorescent pigments. Science. 1969; 166:1535–1536. [PubMed: 17655054]

Chio KS, Tappel AL. Synthesis and characterization of the fluorescent products derived from malonaldehyde and amino acids. Biochem. 1969; 8:2821–2826. [PubMed: 5808334]

Chowdhury PK, Halder M, Choudhury PK, Kraus GA, Desai MJ, Armstrong DW, Casey TA, Rasmussen MA, Petrich JW. Generation of fluorescent adducts of malondialdehyde and amino acids: toward an understanding of lipofuscin. Photochem Photobiol. 2004; 79:21–25. [PubMed: 14974711]

Chrispell JD, Feathers KL, Kane MA, Kim CY, Brooks M, Khanna R, Kurth I, Huebner CA, Gal A, Mears AJ, Swaroop A, Napoli JL, Sparrow JR, Thompson DA. Rdh12 activity and effects on retinoid processing in the murine retina. J Biol Chem. 2009; 284:21468–21477. [PubMed: 19506076]

Cideciyan AV, Swider M, Aleman TS, Tsybovsky Y, Schwartz SB, Windsor EA, Roman AJ, Sumaroka A, Steinberg JD, Jacobson SG, Stone EM, Palczewski K. ABCA4 disease progression and a proposed strategy for gene therapy. Hum Mol Genet. 2009; 18:931–941. [PubMed: 19074458]

Cremers FP, van de Pol DJ, van Driel M, den Hollander AI, van Haren FJ, Knoers NV, Tijmes N, Bergen AA, Rohrschneider K, Blankenagel A, Pinckers AJ, Deutman AF, Hoyng CB. Autosomal recessive retinitis pigmentosa and cone-rod dystrophy caused by splice site mutations in the Stargardt's disease gene ABCR. Hum Mol Genet. 1998; 7:355–362. [PubMed: 9466990]

Del Priore LV, Kuo YH, Tezel TH. Age-related changes in human RPE cell density and apoptosis proportion in situ. Invest Ophthalmol Vis Sci. 2002; 43:3312–3318. [PubMed: 12356840]

Delori FC, Dorey CK, Staurenghi G, Arend O, Goger DG, Weiter JJ. In vivo fluorescence of the ocular fundus exhibits retinal pigment epithelium lipofuscin characteristics. Invest Ophthalmol Vis Sci. 1995; 36:718–729. [PubMed: 7890502]

Delori FC, Fleckner MR, Goger DG, Weiter JJ, Dorey CK. Autofluorescence distribution associated with drusen in age-related macular degeneration. Invest Ophthalmol Vis Sci. 2000; 41:496–504. [PubMed: 10670481]

Delori FC, Goger DG, Dorey CK. Age-related accumulation and spatial distribution of lipofuscin in RPE of normal subjects. Invest Ophthalmol Vis Sci. 2001; 42:1855–1866. [PubMed: 11431454]

Delori FC, Greenberg JP, Woods RL, Fischer J, Duncker T, Sparrow JR, Smith RT. Quantitative measurements of autofluorescence with the scanning laser ophthalmoscope. Invest Ophthalmol Vis Sci. 2011 (in press).

Delori, FC.; Keilhauer, C.; Sparrow, JR.; Staurenghi, G. Origin of fundus autofluorescence. In: Holz, FG.; Schmitz-Valckenberg, S.; Spaide, RF.; Bird, AC., editors. Atlas of Fundus Autofluorescence Imaging. Berlin Heidelberg: Springer-Verlag; 2007. p. 17-29.

Dickinson DA, Forman HJ. Glutathione in defense and signaling. Lessons from a small thiol. Ann N Y Acad Sci. 2002; 973:488–504. [PubMed: 12485918]

Edwards AO, Ritter R, Abel KJ, Manning A, Panhuysen C, Farrer LA. Complement factor H polymorphism and age-related macular degeneration. Science. 2005; 308:421–424. [PubMed: 15761121]

Eldred G, Katz ML. The lipid peroxidation theory of lipofuscinogenesis cannot yet be confirmed. Free Rad Biol Med. 1991; 10:445–447. [PubMed: 1894166]

Eldred GE, Katz ML. The autofluorescent products of lipid peroxidation may not be lipofuscin-like [see comments]. Free Radic Biol Med. 1989; 7:157–163. [PubMed: 2806939]

Eldred GE, Miller GV, Stark WS, Feeney-Burns L. Lipofuscin: resolution of discrepant fluorescence data. Science. 1982; 216:757–758. [PubMed: 7079738]

Farboud B, Aotaki-Keen A, Miyata T, Hjelmeland LM, Handa JT. Development of a polyclonal antibody with broad epitope specificity for advanced glycation endproducts and localization of these epitopes in Bruch's membrane of the aging eye. Mol Vision. 1999; 5:11.

Feeney-Burns L, Eldred GE. The fate of the phagosome: conversion to 'age pigment' and impact in human retinal pigment epithelium. Trans Ophthalmol Soc U K. 1983; 103:416–421. [PubMed: 6589859]

Ferri G, Comerio G, Iadarola P, Zapponi MC, Speranza ML. Subunit structure and activity of glyceraldehyde-3-phosphate dehydrogenase from spinach chloroplasts. Biochim Biophys Acta. 1978; 522:19–31. [PubMed: 23161]

Field MG, Elner VM, Puro DG, Feuerman JM, Musch DC, Pop-Busui R, Hackel R, Heckenlively JR, Petty HR. Rapid, noninvasive detection of diabetes-induced retinal metabolic stress. Arch Ophthalmol. 2008; 126:934–938. [PubMed: 18625939]

Fishkin N, Jang YP, Itagaki Y, Sparrow JR, Nakanishi K. A2-rhodopsin: a new fluorophore isolated from photoreceptor outer segments. Org Biomol Chem. 2003; 1:1101–1105. [PubMed: 12926382]

Fishkin N, Sparrow JR, Allikmets R, Nakanishi K. Isolation and characterization of a retinal pigment epithelial cell fluorophore: an all-trans-retinal dimer conjugate. Proc Natl Acad Sci U S A. 2005; 102:7091–7096. [PubMed: 15870200]

Fliesler SJ, Anderson RE. Chemistry and metabolism of lipids inthe vertebrate retina. Prog Lipid Res. 1983; 22:79–131. [PubMed: 6348799]

Gaillard ER, Atherton SJ, Eldred G, Dillon J. Photophysical studies on human retinal lipofuscin. Photochem Photobiol. 1995; 61:448–453. [PubMed: 7770505]

Glenn JV, Beattie JR, Barrett L, Frizzell N, Thorpe SR, Boulton ME, McGarvey JJ, Stitt AW. Confocal raman microscopy can quantify advanced glycation end product (AGE) modification in Bruch's membrane leading to accurate nondestructive prediction of ocular aging. FASEB J. 2007; 21:3542–3552. [PubMed: 17567569]

Golczak M, Kuksa V, Maeda T, Moise AR, Palczewski K. Positively charged retinoids are potent and selective inhibitors of the trans-cis isomerization in the retinoid (visual) cycle. Proc Natl Acad Sci U S A. 2005 Jun 7; 102(23):8162–8167. 2005. [PubMed: 15917330]

Grayson C, Molday RS. Dominant negative mechanism underlies autosomal dominant Stargardt-like macular dystrophy linked to mutations in ELOVL4. J Biol Chem. 2005; 280:32521–32530. [PubMed: 16036915]

Grey AC, Crouch RK, Koutalos Y, Schey KL, Ablonczy Z. Spatial localization of A2E in the retinal pigment epithelium. Invest Ophthalmol Vis Sci. 2011; 52:3926–3933. [PubMed: 21357388]

Hageman GS, Anderson DH, Johnson LV, Hancox LS, Taiber AJ, Hardisty LI, Hageman JL, Stockman HA, Borchardt JD, Gehrs KM, Smith RJH, Silvestri G, Russell SR, Klaver CCW, Barbazetto I, Chang S, Yannuzzi LA, Barile GR, Merriam JC, Smith RT, Olsh AK, Bergeron J, Zernant J, Merriam JE, Gold B, Dean M, Allikmets R. A common haplotype in the complement regulatory gene factor H (HF1/CFH) predisposes individuals to age-related macular degeneration. Proc Natl Acad Sci U S A. 2005; 102:7227–7232. [PubMed: 15870199]

Haines JL, Hauser MA, Schmidt S, Scott WK, Olson LM, Gallins P, Spencer KL, Kwan SY, Noureddine M, Gilbert JR, Schnetz-Boutaud N, Agarwal A, Postel EA, Pericak-Vance MA. Complement factor H variant increases the risk of age-related macular degeneration. Science. 2005; 308:419–421. [PubMed: 15761120]

Handa JT, Verzijl N, Matsunaga H, Aotaki-Keen A, Lutty GA, Koppele JM, Miyata T, Hjelmeland LM. Increase in advanced glycation end product pentosidine in Bruch's membrane with age. Invest Ophthalmol Vis Sci. 1999; 40:775–779. [PubMed: 10067983]

Holz FG, Bellman C, Staudt S, Schutt F, Volcker HE. Fundus autofluorescence and development of geographic atrophy in age-related macular degeneration. Invest Ophthalmol Vis Sci. 2001; 42:1051–1056. [PubMed: 11274085]

Hunter JJ, Morgan JIW, Merigan WH, Sliney DH, Sparrow JR, Williams DR. The susceptibility of the retina to light damage. Prog Retina Eye Res. 2011 in press.

Ishibashi T, Murata T, Hangai M, Nagai R, Horiuchi S, Lopez PF, Hinton DR, Ryan SJ. Advanced glycation end products in age-related macular degeneration. Arch Ophthalmol. 1998; 116:1629–1632. [PubMed: 9869793]

Janecke AR, Thompson DA, Utermann G, Becker C, Hübner CA, Schmid E, McHenry CL, Nair AR, Rüschendorf F, Heckenlively JR, Wissinger B, Nürnberg P, Gal A. Mutations in RDH12 encoding a photoreceptor cell retinol dehydrogenase cause childhood-onset severe retinal dystrophy. Nat Genet. 2004; 36:850–854. [PubMed: 15258582]

Jang YP, Matsuda H, Itagaki Y, Nakanishi K, Sparrow JR. Characterization of peroxy-A2E and furan-A2E photooxidation products and detection in human and mouse retinal pigment epithelial cells lipofuscin. J Biol Chem. 2005; 280:39732–39739. [PubMed: 16186115]

Jin ML, Li S, Moghrabi WN, Sun H, Travis GH. Rpe65 is the retinoid isomerase in bovine retinal pigment epithelium. Cell. 2005; 122:449–459. [PubMed: 16096063]

Justilien V, Pang JJ, Renganathan K, Zhan X, Crabb JW, Kim SR, Sparrow JR, Hauswirth WW, Lewin AS. SOD2 knockdown mouse model of early AMD. Invest Ophthalmol Vis Sci. 2007; 48:4407–4420. [PubMed: 17898259]

Kanofsky JR, Sima PD, Richter C. Singlet-oxygen generation from A2E. Photochem Photobiol. 2003; 77:235–242. [PubMed: 12685649]

Karan G, Lillo C, Yang Z, Cameron DJ, Locke KG, Zhao Y, Thirumalaichary S, Li C, Birch DG, Vollmer-Snarr HR, Williams DS, Zhang K. Lipofuscin accumulation, abnormal electrophysiology, and photoreceptor degeneration in mutant ELOVL4 transgenic mice: a model for macular degeneration. Proc Natl Acad Sci U S A. 2005a; 102:4164–4169. [PubMed: 15749821]

Karan G, Yang Z, Howes K, Zhao Y, Chen Y, Cameron DJ, Lin Y, Pearson E, Zhang K. Loss of ER retention and sequestration of the wild-type ELOVL4 by Stargardt disease dominant negative mutants. Mol Vision. 2005b; 11:657–664.

Katz ML, Drea CM, Eldred GE, Hess HH, Robison WG Jr. Influence of early photoreceptor degeneration on lipofuscin in the retinal pigment epithelium. Exp Eye Res. 1986; 43:561–573. [PubMed: 3792460]

Katz ML, Eldred GE, Robison WG Jr. Lipofuscin autofluorescence: evidence for vitamin A involvement in the retina. Mech Ageing Dev. 1987; 39:81–90. [PubMed: 3613689]

Katz ML, Redmond TM. Effect of Rpe65 knockout on accumulation of lipofuscin fluorophores in the retinal pigment epithelium. Invest Ophthalmol Vis Sci. 2001; 42:3023–3030. [PubMed: 11687551]

Kim SR, Fishkin N, Kong J, Nakanishi K, Allikmets R, Sparrow JR. The Rpe65 Leu450Met variant is associated with reduced levels of the RPE lipofuscin fluorophores A2E and iso-A2E. Proc Natl Acad Sci U S A. 2004; 101:11668–11672. [PubMed: 15277666]

Kim SR, He J, Yanase E, Jang YP, Berova N, Sparrow JR, Nakanishi K. Characterization of dihydro-A2PE: an Intermediate in the A2E biosynthetic pathway. Biochem. 2007a; 46:10122–10129. [PubMed: 17685561]

Kim SR, Jang YP, Jockusch S, Fishkin NE, Turro NJ, Sparrow JR. The all-trans-retinal dimer series of lipofuscin pigments in retinal pigment epithelial cells in a recessive Stargardt disease model. Proc Natl Acad Sci U S A. 2007b; 104:19273–19278. [PubMed: 18048333]

Kindzewlskii A, Petty HR. Fluorescence spectroscopic detection of mitochondrial flavoprotein redox oscillations and transient reduction of the NADPH oxidase-associated flavoprotein in leukocytes. Eur Biophys J. 2004; 33:291–299. [PubMed: 14574524]

Klein RJ, Zeiss C, Chew EY, Tsai JY, Sackler RS, Haynes C, Henning AK, SanGiovanni JP, Mane SM, Mayne ST, Bracken MB, Ferris FL, Ott J, Barnstable C, Hoh J. Complement factor H

polymorphism in age-related macular degeneration. Science. 2005; 308:385–389. [PubMed: 15761122]

Kong J, Kim SR, Binley K, Pata, Doi K, Mannik J, Zernant-Rajang J, Kan O, Iqball S, Naylor S, Sparrow JR, Gouras P, Allikmets R. Correction of the disease phenotype in the mouse model of Stargardt disease by lentiviral gene therapy. Gene Ther. 2008; 15:1311–1320. [PubMed: 18463687]

Lamb LE, Ye T, Haralampus-Grynaviski NM, Williams TR, Pawlak A, Sarna T, Simon JD. Primary photophysical properties of A2E in solution. J Phys Chem B. 2001; 105:11507–11512.

Lee HJ, Howell SK, Sanford RJ, Beisswenger PJ. Methylglyoxal can modify GAPDH activity and structure. Ann NY Acad Sci. 2005; 1043:135–145. [PubMed: 16037232]

Liu J, Itagaki Y, Ben-Shabat S, Nakanishi K, Sparrow JR. The biosynthesis of A2E, a fluorophore of aging retina, involves the formation of the precursor, A2-PE, in the photoreceptor outer segment membrane. J Biol Chem. 2000; 275:29354–29360. [PubMed: 10887199]

Lois N, Owens SL, Coco R, Hopkins J, Fitzke FW, Bird AC. Fundus autofluorescence in patients with age-related macular degeneration and high risk of visual loss. Am J Ophthalmol. 2002; 133:341–349. [PubMed: 11860971]

Lorenz B, Wabbels B, Wegscheider E, Hamel CP, Drexler W, Presing MN. Lack of fundus autofluorescence to 488 nanometers from childhood on in patients with early-onset severe retinal dystrophy associated with mutations in RPE65. Ophthalmol. 2004; 111:1585–1594.

Lyubarsky AL, Savchenko AB, Morocco SB, Daniele LL, Redmond TM, Pugh EN. Mole quantity of RPE65 and its productivity in the generation of 11-cis-retinal from retinyl esters in the living mouse eye. Biochem. 2005; 44:9880–9888. [PubMed: 16026160]

Maeda A, Maeda T, Golczak M, Palczewski K. Retinopathy in mice induced by disrupted all-trans-retinal clearance. J Biol Chem. 2008; 283:26684–26693. [PubMed: 18658157]

Maiti P, Kong J, Kim SR, Sparrow JR, Allikmets R, Rando RR. Small molecule RPE65 antagonists limit the visual cycle and prevent lipofuscin formation. Biochem. 2006; 45:852–860. [PubMed: 16411761]

Majji AB, Cao J, Chang KY, Hayashi A, Aggarwal S, Grebe RR, de Juan E. Invest Ophthalmol Vis Sci. 2000; 52:3936–3942. [PubMed: 11053297]

Marmorstein AD, Marmorstein LY, Sakaguchi H, Hollyfield JG. Spectral profiling of autofluorescence associated with lipofuscin, Bruch's Membrane, and sub-RPE deposits in normal and AMD eyes. Invest Ophthalmol Vis Sci. 2002; 43:2435–2441. [PubMed: 12091448]

Mata NL, Weng J, Travis GH. Biosynthesis of a major lipofuscin fluorophore in mice and humans with ABCR-mediated retinal and macular degeneration. Proc Natl Acad Sci U S A. 2000; 97:7154–7159. [PubMed: 10852960]

Michaelides, M. Fundus autofluorescence in cone and cone-rod dystrophies. In: Lois, N.; Forrester, JV., editors. Fundus Autofluorescence. Philadelphia: Lippincott Williams and Wilkins; 2009. p. 153-166.

Moiseyev G, Chen Y, Takahashi Y, Wu BX, Ma JX. RPE65 is the isomerohydrolase in the retinoid visual cycle. Proc Natl Acad Sci U S A. 2005; 102:12413–12418. [PubMed: 16116091]

Molday LL, Rabin AR, Molday RS. ABCR expression in foveal cone photoreceptors and its role in Stargardt macular dystrophy. Nat Genet. 2000; 25:257–258. [PubMed: 10888868]

Molday RS, Molday LL. Identification and characterization of multiple forms of rhodopsin and minor proteins in frog and bovine outer segment disc membranes. Electrophoresis, lectin labeling and proteolysis studies. J Biol Chem. 1979; 254:4653–4660. [PubMed: 312291]

Molday RS, Zhong M, Quazi F. The role of the photoreceptor ABC transporter ABCA4 in lipid transport and Stargardt macular degeneration. Biochimica et Biophysica Acta. 2009; 1791:573–583. [PubMed: 19230850]

Morgan JI, Dubra A, Wolfe R, Merigan WH, Williams DR. In vivo autofluorescence imaging of the human and macaque retinal pigment epithelial cell mosaic. Invest Ophthalmol Vis Sci. 2009; 50:1350–1359. [PubMed: 18952914]

Ng KP, Gugiu BG, Renganathan K, Davies MW, Gu X, Crabb JS, Kim SR, Rozanowska MB, Bonilha VL, Rayborn ME, Salomon RG, Sparrow JR, Boulton ME, Hollyfield JG, Crabb JW. Retinal

pigment epithelium lipofuscin proteomics. Mol Cell Proteomics. 2008; 7:1397–1405. [PubMed: 18436525]

Nomura, Y.; Takeda, T.; Okuma, Y. The Senescence-Accelerated Mouse (SAM): An Animal Model of Senescence. Amsterdam, The Netherlands: Elsevier B.V.; 2004.

Nusinowitz S, Nguyen L, Radu RA, Kashani Z, Farber DB, Danciger M. Electroretinographic evidence for altered phototransduction gain and slowed recovery from photobleaches in albino mice with a MET450 variant in RPE6. Exp Eye Res. 2003; 77:627–638. [PubMed: 14550405]

Papermaster DS, Schneider BG, Zorn MA, Kraehenbuhl JP. Immunocytochemical localization of a large intrinsic membrane protein to the incisures and margins of frog rod outer segment disks. J Cell Biol. 1978; 78:415–425. [PubMed: 690173]

Parish CA, Hashimoto M, Nakanishi K, Dillon J, Sparrow JR. Isolation and one-step preparation of A2E and iso-A2E, fluorophores from human retinal pigment epithelium. Proc Natl Acad Sci U S A. 1998; 95:14609–14613. [PubMed: 9843937]

Pawar AS, Qtaishat NM, Little DM, Pepperberg DR. Recovery of rod photoresponses in ABCR-deficient mice. Invest Ophthalmol Vis Sci. 2008; 49:2743–2755. [PubMed: 18263807]

Pawlak A, Rozanowska M, Zareba M, Lamb LE, Simon JD, Sarna T. Action spectra for the photoconsumptioin of oxygen by human ocular lipofuscin and lipofuscin extracts. Arch Biochem Biophys. 2002; 403:59–62. [PubMed: 12061802]

Pawlak A, Wrona M, Rozanowska M, Zareba M, Lamb LE, Roberts JE, Simon JD, Sarna T. Comparison of the aerobic photoreactivity of A2E with its precursor retinal. Photochem Photobiol. 2003; 77:253–258. [PubMed: 12685651]

Poincelot RP, Millar PG, Kimbel RL Jr, Abrahamson EW. Lipid to protein chromophore transfer in the photolysis of visual pigments. Nature. 1969; 221:256–257. [PubMed: 5763079]

Radu RA, Hu J, Yuan Q, Welch DL, Makshanoff J, Lloyd M, McMullen S, Travis GH, Bok D. Complement system dysregulation and inflammation in the retinal pigment epithelium of a mouse model for Stargardt macular degeneration. J Biol Chem. 2011; 286:18593–18601. [PubMed: 21464132]

Radu RA, Yuan Q, Hu J, Peng JH, Lloyd M, Nusinowitz S, Bok D, Travis GH. Accelerated accumulation of lipofuscin pigments in the RPE of a mouse model for ABCA4-mediated retinal dystrophies following Vitamin A supplementation. Invest Ophthalmol Vis Sci. 2008; 49:3821–3829. [PubMed: 18515570]

Redmond TM, Poliakov E, Yu S, Tsai JY, Lu Z, Gentleman S. Mutation of key residues of RPE65 abolishes its enzymatic role as isomerohydrolase in the visual cycle. Proc Natl Acad Sci U S A. 2005; 102:13658–13663. [PubMed: 16150724]

Rein D, Tappel AL. Fluorescent lipid oxidation products and heme spectra index antioxidant efficacy in kidney tissue of hamsters. Free Radic Biol Med. 1998; 24:1278–1284. [PubMed: 9626584]

Reszka K, Eldred GE, Wang RH, Chignell C, Dillon J. The photochemistry of human retinal lipofuscin as studied by EPR. Photochem Photobiol. 1995; 62:1005–1008. [PubMed: 8570736]

Roberts JE, Kukielczak BM, Hu DN, Miller DS, Bilski P, Sik RH, Motten AG, Chignell CF. The role of A2E in prevention or enhancement of light damage in human retinal pigment epithelial cells. Photochem Photobiol. 2002; 75:184–190. [PubMed: 11883606]

Robson AG, Michaelides M, Luong VA, Holder GE, Bird AC, Webster AR, Moore AT, Fitzke FW. Functional correlates of fundus autofluorescence abnormalities in patients with RPGR or RIMS1 mutations causing cone or cone rod dystrophy. Br J Ophthalmol. 2008a; 92:95–102. [PubMed: 17962389]

Robson AG, Michaelides M, Saihan Z, Bird AC, Webster AR, Moore AT, Fitzke FW, Holder GE. Functional characteristics of patients with retinal dystrophy that manifest abnormal parafoveal annuli of high density fundus autofluorescence: a review and update. Doc Ophthalmol. 2008b; 116:79–89. [PubMed: 17985165]

Rozanowska M, Jarvis-Evans J, Korytowski W, Boulton ME, Burke JM, Sarna T. Blue light-induced reactivity of retinal age pigment. In vitro generation of oxygen-reactive species. J Biol Chem. 1995; 270:18825–18830. [PubMed: 7642534]

Rozanowska M, Korytowski W, Rozanowska B, Skumatz C, Boulton ME, Burke JM, Sarna T. Photoreactivitiy of aged human RPE melanosomes: a comparison with lipofuscin. Invest Ophthalmol Vis Sci. 2002; 43:2088–2096. [PubMed: 12091401]

Rozanowska M, Pawlak A, Rozanowska B, Skumatz C, Zareba M, Boulton ME, Burke JM, Sarna T, Simon JD. Age-related changes in the photoreactivity of retinal lipofuscin granules: role of chloroform-insoluble components. Invest Ophthalmol Vis Sci. 2004; 45:1052–1060. [PubMed: 15037568]

Rozanowska M, Wessels J, Boulton M, Burke JM, Rodgers MAJ, Truscott TG, Sarna T. Blue light-induced singlet oxygen generation by retinal lipofuscin in non-polar media. Free Rad Biol Med. 1998; 24:1107–1112. [PubMed: 9626564]

Schutt F, Davies S, Kopitz J, Holz FG, Boulton ME. Photodamage to human RPE cells by A2-E, a retinoid component of lipofuscin. Invest Ophthalmol Vis Sci. 2000; 41:2303–2308. [PubMed: 10892877]

Schutt F, Ueberle B, Schnolzer M, Holz FG, Kopitz J. Proteome analysis of lipofuscin in human retinal pigment epithelial cells. FEBS Lett. 2002; 528:217–221. [PubMed: 12297308]

Shroyer NF, Lewis RA, Allikmets R, Singh N, Dean M, Leppert M, Lupski JR. The rod photoreceptor ATP-binding cassette transporter gene, ABCR, and retinal disease: from monogenic to multifactorial. Vision Res. 1999; 39:2537–2544. [PubMed: 10396622]

Sparrow, JR. Lipofuscin of the retinal pigment epithelium. In: Holz, FG.; Schmitz-Valckenberg, S.; Spaide, RF.; Bird, AC., editors. Atlas of Autofluorescence Imaging. Heidelberg: Springer; 2007a. p. 3-16.

Sparrow, JR. RPE lipofuscin: formation, properties and relevance to retinal degeneration. In: Tombran-Tink, J.; Barnstable, CJ., editors. Retinal Degenerations: Biology, Diagnostics and Therapeutics. Totowa, NJ: Humana Press; 2007b. p. 213-236.

Sparrow JR, Kim SR, Cuervo AM, Bandhyopadhyayand U. A2E, a pigment of RPE lipofuscin is generated from the precursor A2PE by a lysosomal enzyme activity. Adv Exp Med and Biol. 2008; 613:393–398. [PubMed: 18188969]

Sparrow JR, Nakanishi K, Parish CA. The lipofuscin fluorophore A2E mediates blue light-induced damage to retinal pigmented epithelial cells. Invest Ophthalmol Vis Sci. 2000; 41:1981–1989. [PubMed: 10845625]

Sparrow JR, Parish CA, Hashimoto M, Nakanishi K. A2E, a lipofuscin fluorophore, in human retinal pigmented epithelial cells in culture. Invest Ophthalmol Vis Sci. 1999; 40:2988–2995. [PubMed: 10549662]

Sparrow JR, Wu Y, Kim CY, Zhou J. Phospholipid meets all-*trans*-retinal: the making of RPE bisretinoids. J. Lipid Res. 2010a; 51:247–261. [PubMed: 19666736]

Sparrow JR, Wu Y, Nagasaki T, Yoon KD, Yamamoto K, Zhou J. Fundus autofluorescence and the bisretinoids of retina. Photochem Photobiol Sci. 2010b; 9:1480–1489. [PubMed: 20862444]

Sparrow JR, Yoon K, Wu Y, Yamamoto K. Interpretations of fundus autofluorescence from studies of the bisretinoids of retina. Invest Ophthalmol Vis Sci. 2010c; 51:4351–4357. [PubMed: 20805567]

Sparrow JR, Zhou J, Ben-Shabat S, Vollmer H, Itagaki Y, Nakanishi K. Involvement of oxidative mechanisms in blue light induced damage to A2E-laden RPE. Invest Ophthalmol Vis Sci. 2002; 43:1222–1227. [PubMed: 11923269]

Sun H, Molday RS, Nathans J. Retinal stimulates ATP hydrolysis by purified and reconstituted ABCR, the photoreceptor-specific ATP-binding cassette transporter responsible for Stargardt disease. J Biol Chem. 1999; 274:8269–8281. [PubMed: 10075733]

Sun H, Nathans J. Stargardt's ABCR is localized to the disc membrane of retinal rod outer segments. Nat Genet. 1997; 17:15–16. [PubMed: 9288089]

Sun H, Nathans J. ABCR, the ATP-binding cassette transporter responsible for Stargardt macular dystrophy, is an efficient target of all-trans retinal-mediated photo-oxidative damage in vitro: implications for retinal disease. J Biol Chem. 2001a; 276:11766–11774. [PubMed: 11278627]

Sun H, Nathans J. Mechanistic studies of ABCR, the ABC transporter in photoreceptor outer segments responsible for autosomal recessive Stargardt disease. J Bioenerg Biomembrane. 2001b; 33:523–530. [PubMed: 11804194]

Szamier RB, Berson EL. Retinal ultrastructure in advanced retinitis pigmentosa. Invest Ophthalmol Vis Sci. 1977; 16:947–962. [PubMed: 908648]

Tanito M, Brush RS, Elliott MH, Wicker LD, Henry KR, Anderson RE. High levels of retinal membrane docosahexaenoic acid increase susceptibility to stress-induced degeneration. J Lipid Res. 2009; 50:807–819. [PubMed: 19023138]

Vasireddy V, Jablonski MM, Khan NW, Wang XF, Sahu P, Sparrow JR, Ayyagari R. Elovl4 5-bp deletion knock-in mouse model for Stargardt-like macular degeneration demonstrates accumulation of ELOVL4 and lipofusin. Exp Eye Research. 2009; 89:905–912.

Vasireddy V, Vijayasarathy C, Huang J, Wang XF, Jablonski MM, Petty HR, Sieving PA, Ayyagari R. Stargardt-like macular dystrophy protein ELOVL4 exerts a dominant negative effect by recruiting wild-type protein into aggresomes. Mol Vision. 2005; 11:665–676.

von Ruckmann A, Fitzke FW, Bird AC. Fundus autofluorescence in age-related macular disease imaged with a laser scanning ophthalmoscope. Invest Ophthalmol Vis Sci. 1997; 38:478–486. [PubMed: 9040481]

Warburton S, Southwick K, Hardman RM, Secrest AM, Grow RK, Xin H, Woolley AT, Burton GF, Thulin CD. Examining the proteins of functional retinal lipofuscin using proteomic analysis as a guide for understanding its origin. Mol Vis. 2005; 11:1122–1134. [PubMed: 16379024]

Weiter JJ, Delori FC, Wing GL, Fitch KA. Retinal pigment epithelial lipofuscin and melanin and choroidal melanin in human eyes. Invest Ophthalmol Vis Sci. 1986; 27:145–151. [PubMed: 3943941]

Weng J, Mata NL, Azarian SM, Tzekov RT, Birch DG, Travis GH. Insights into the function of Rim protein in photoreceptors and etiology of Stargardt's disease from the phenotype in abcr knockout mice. Cell. 1999; 98:13–23. [PubMed: 10412977]

Wing GL, Blanchard GC, Weiter JJ. The topography and age relationship of lipofuscin concentration in the retinal pigment epithelium. Invest Ophthalmol Vis Sci. 1978; 17:601–607. [PubMed: 669891]

Wu L, Nagasaki T, Sparrow JR. Photoreceptor cell degeneration in*Abcr*$^{-/-}$mice. Adv Exp Med Biol. 2010a; 664:533–539. [PubMed: 20238056]

Wu Y, Fishkin NE, Pande A, Pande J, Sparrow JR. Novel lipofuscin bisretinoids prominent in human retina and in a model of recessive Stargardt disease. J Biol Chem. 2009; 284:20155–20166. [PubMed: 19478335]

Wu Y, Yanase E, Feng X, Siegel MM, Sparrow JR. Structural characterization of bisretinoid A2E photocleavage products and implications for age-related macular degeneration. Proc Natl Acad Sci. 2010b; 107:7275–7280. [PubMed: 20368460]

Yamamoto K, Yoon KD, Ueda K, Hashimoto M, Sparrow JR. A novel bisretinoid of retina is an adduct on glycerophosphoethanolamine. Invest Ophthalmol Vis Sci. 2012 (in press).

Zhang K, Kniazeva M, Han M, Li W, Yu Z, Yang Z, Li Y, Metzker ML, Allikmets R, Zack DJ, Kakuk LE, Lagali PS, Wong PW, MacDonald IM, Sieving PA, Figueroa DJ, Austin CP, Gould RJ, Ayyagari R, Petrukhin K. A 5-bp deletion in ELOVL4 is associated with two related forms of autosomal dominant macular dystrophy. Nat Genet. 2001; 27:89–93. [PubMed: 11138005]

Zhong M, Molday LL, Molday RS. Role of the C terminus of the photoreceptor ABCA4 transporter in protein folding, function and retinal degenerative disease. J Biol Chem. 2009; 284:3640–3649. [PubMed: 19056738]

Zhou J, Jang YP, Kim SR, Sparrow JR. Complement activation by photooxidation products of A2E, a lipofuscin constituent of the retinal pigment epithelium. Proc Natl Acad Sci U S A. 2006; 103:16182–16187. [PubMed: 17060630]

Zhou J, Kim SR, Westlund BS, Sparrow JR. Complement activation by bisretinoid constituents of RPE lipofuscin. Invest Ophthalmol Vis Sci. 2009; 50:1392–1399. [PubMed: 19029031]

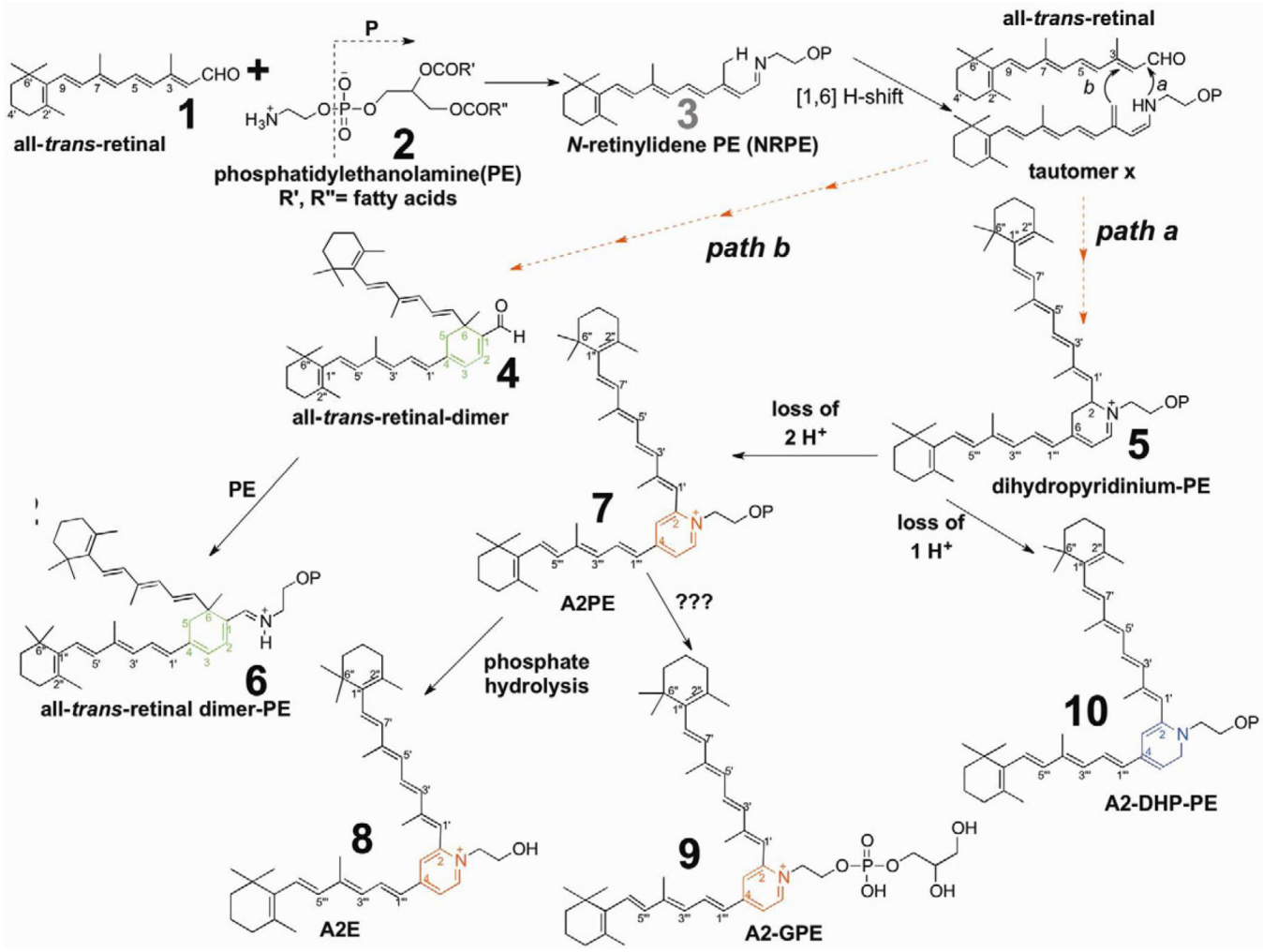

Figure 1.

Proposed biosynthetic schemes for bisretinoid formation. All-*trans*-retinal that is released from opsin after photoisomerization of ground state 11-*cis*-retinal reacts with phosphatidylethanolamine (PE) in the disk membrane to produce the *N*-retinyl-phosphatidylethanolamine Schiff base (NRPE). NRPE undergoes a [1,6] H-shift producing tautomer X. Reaction with a second molecule of all-*trans*-retinal leads to path **a** and the formation of a bisretinoid phosphatidyl-dihydropyridinium molecule (dihydropyridinium-A2PE). Dihydropyridinium-A2PE automatically loses one hydrogen to produce A2-dihydropyridine-phosphatidylethanolamine (A2-DHP-PE) or it can eliminate 2 hydrogens to form A2PE, a phosphatidyl-pyridinium bis-retinoid. Hydrolysis of the phosphate ester of A2PE, probably by the lysosomal enzyme phospholipase D, yields A2E. Alternatively, all-*trans*-retinal can add to tautomer × and after ring closure all-*trans*-retinal dimer will form (path **b**). Subsequent Schiff base reaction with PE yields all-*trans*-retinal dimer-PE. Dashed arrows indicate multiple steps in the pathway. Note that OP indicates retention of phosphatidic acid (glycerol, phosphate and fatty acids) originating from PE.

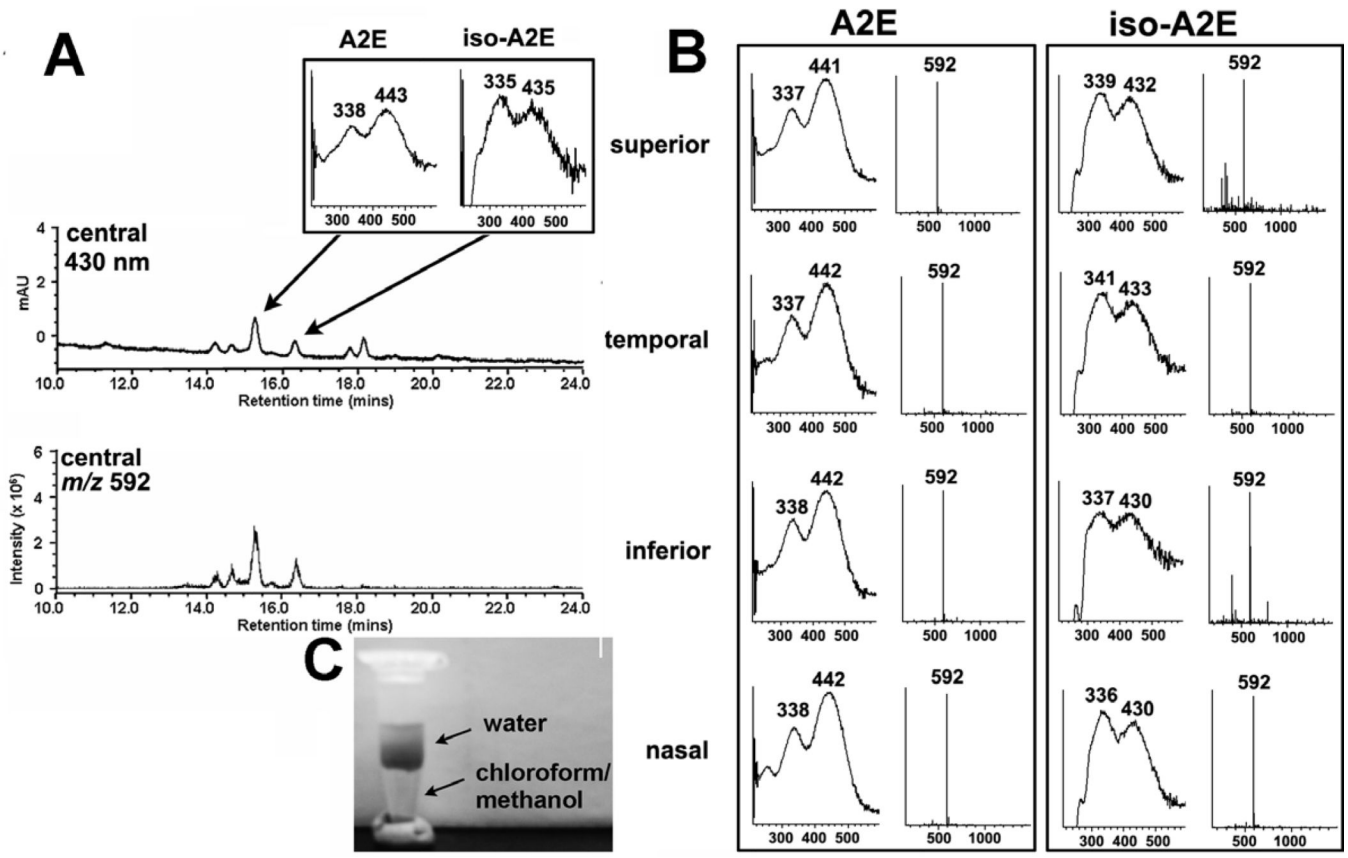

Figure. 2.

A2E accumulates in central and peripheral retina of adult human eye. RPE/choroid samples obtained from human eye using 4 mm trephine. **A**. RPE/choroid from central (centered on fovea) retina. Tissue was analyzed by ultra performance liquid chromatography/mass spectrometry (MS) analysis (electrospray ion multi-mode ionization, ESI). *Upper trace*, chromatogram with absorbance monitoring at 430 nm. *Inset*, absorbance spectra of A2E and isoA2E. *Lower trace*, ESI-MS at *m/z* 592, the molecular weight of A2E. **B**. RPE/choroid from each of four retinal quadrants. Shown are absorbance spectra and molecular weights (*m/z*) for A2E and isoA2E obtained by analysis of samples from each quadrant. **C**. Chloroform/methanol extract of human RPE/choroid showing water soluble and chloroform/methanol soluble phases.

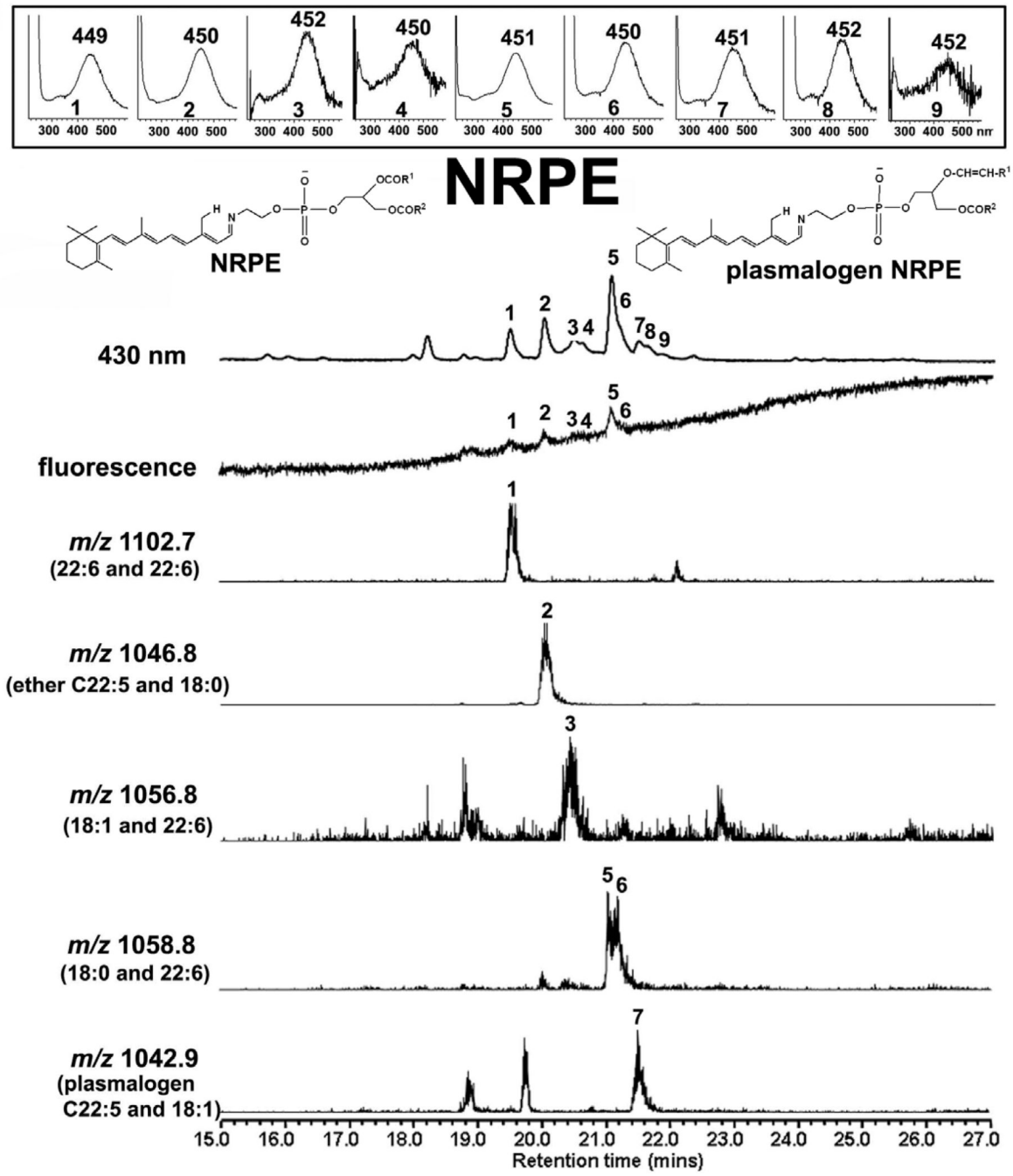

Figure 3.

Ultra performance liquid chromatography/mass spectrometry analysis (electrospray ion multi-mode ionization) of eyes obtained from *Abca4*$^{-/-}$ mice (2–3 months of age, 8 eyes) with detection of *N*-retinylidene-PE (NRPE), the Schiff base adduct of all-*trans*-retinal and phosphatidylethanolamine. UPLC operated with BEH phenyl™ C18 reversed phase column with a mobile phase of acetonitrile/methanol (1:1) in water with 0.1% formic acid. Monitoring of 430 nm absorbance, fluorescence and molecular weight (*m/z*). NRPE is detected as multiple peaks reflecting differences in length of fatty acid chains and in unsaturation. The derived *m/z* values correspond to the lipid moieties indicated in parentheses. *Insets* above, UV-visible absorbance spectra of indicated eluting compounds.

Structures, NRPE and plasmalogen-NRPE. NRPE has the usual ester bonds at the carbon 1 (*sn*-1) and carbon 2 (*sn*-2) positions of glycerol. In plasmalogen-NRPE the first position of the glycerol backbone is bonded to a vinyl-ether moiety (i.e. a carbon-carbon double bond on one side of a ether (C-O-C) linkage).

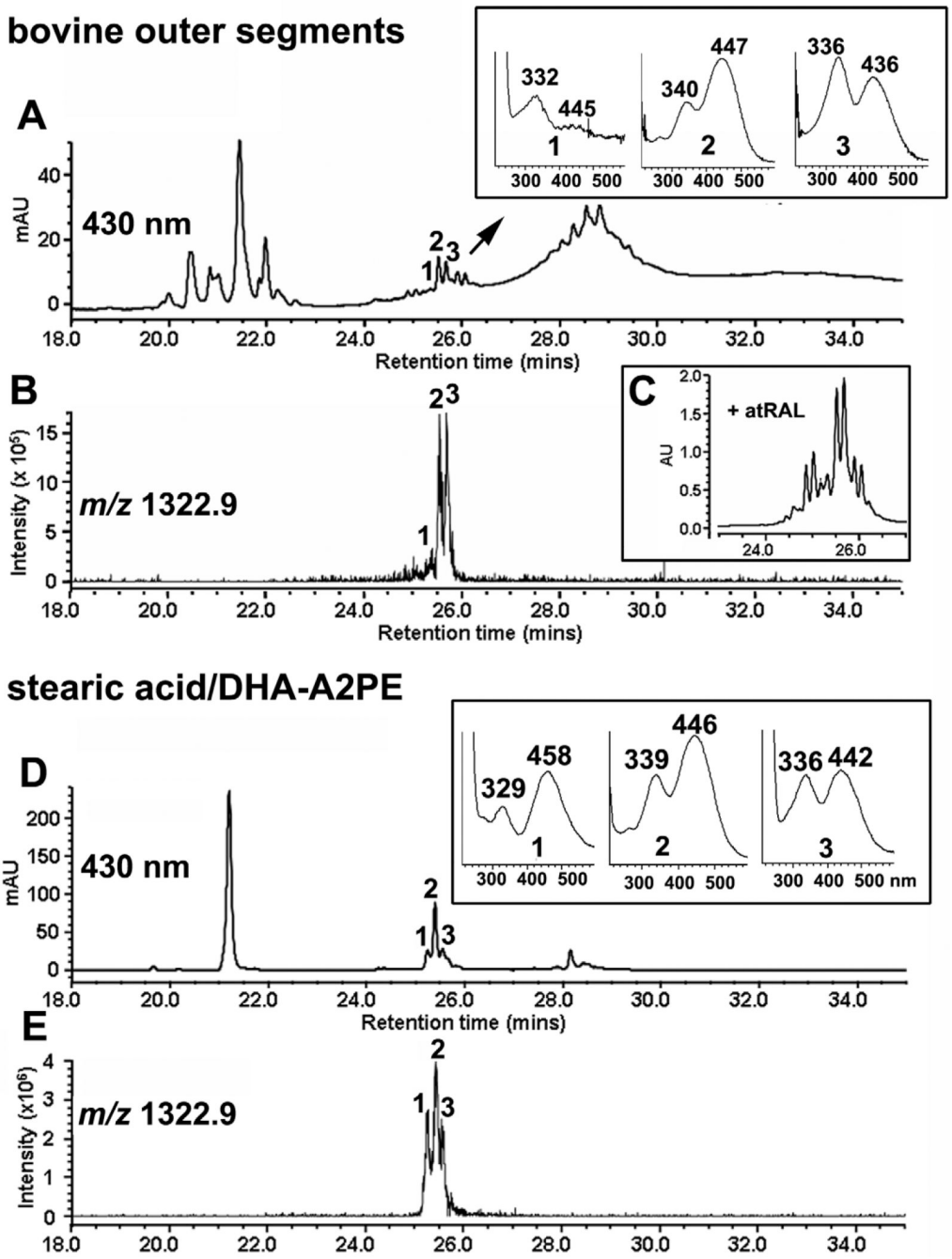

Figure 4.

Detection of the bisretinoid A2PE in isolated bovine photoreceptor outer segments (POS). Ultra performance liquid chromatography/mass spectrometry analysis (electrospray ion multi-mode ionization) as in Fig. 2. **A and B**. In POS extract, a series of chromatographic peaks (A) exhibit *m/z* 1322.9 (B). UV-visible absorbances (*Insets in A*) are consistent with A2PE; the multiple peaks with same *m/z* are indicative of A2PE isomers. **C**. Incubation of POS with all-*trans*-retinal accentuates peak height (peaks 1–3 in A are increased in C), indicating that peaks 1–3 reflect compounds forming by reaction of all-*trans*-retinal. **D and E.** The fatty acid species in the A2PE detected in POS (A) are identified as stearic acid (18:0) and docosahexaenoic acid (DHA, 22:6) since A2PE synthesized from 1-stearoyl-2-

docosahexaenoyl-*sn*-glycero-3-phosphoethanolamine has the same retention time (D) and m/z (E) as the compound in A and B.

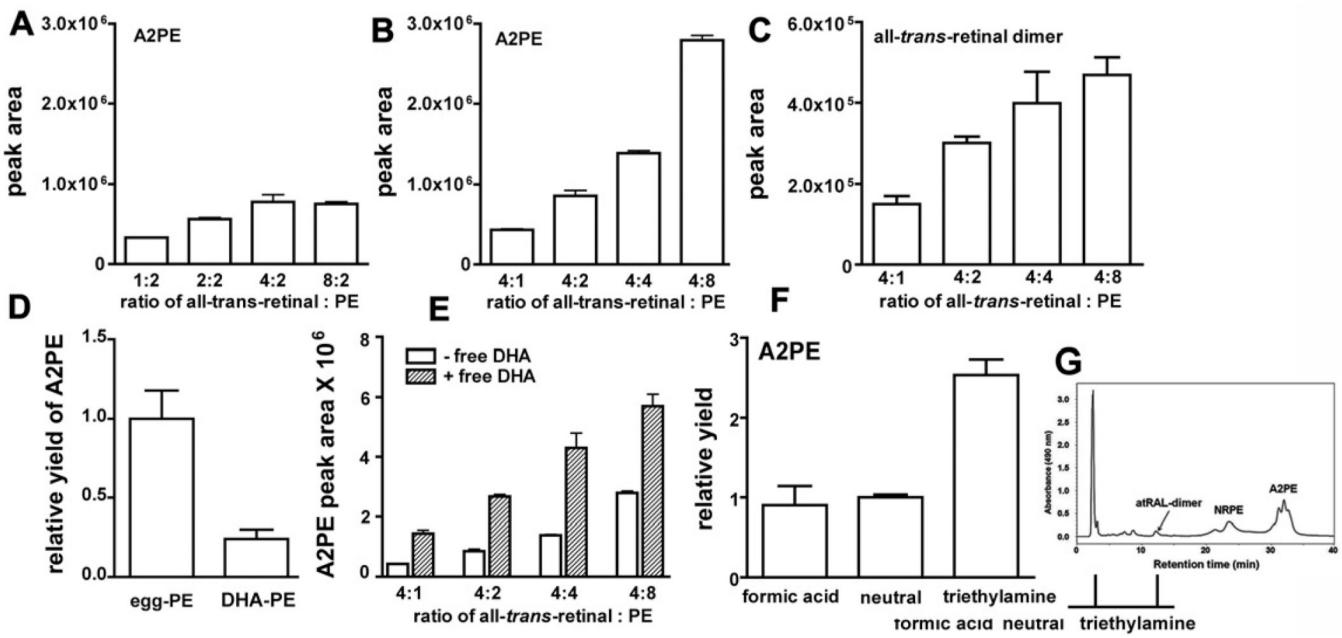

Figure 5.

A2PE and all-*trans*-retinal dimer synthesis: modulating factors. Reaction mixtures of all-*trans*-retinal and phosphatidylethanolamine (PE). Presented as equivalent ratios. **A**. A2PE formation when concentration of all-*trans*-retinal is varied. **B**. A2PE formation when concentration of PE is varied. **C**. All-*trans*-retinal dimer synthesis with varying PE concentration. **D**. A2PE yield using egg yolk-PE versus docosahexaenoic-PE (DHA-PE) as precursor. **E**. A2PE yield with varying levels of egg-PE and in the presence/absence of free DHA fatty acid (8 equivalents). **F**. A2PE yield is facilitated in presence of triethylamine; all-*trans*-retinal:PE ratio was 4:2. Synthetic reaction mixtures were prepared in chloroform/methanol (3:1) at 37°C. **G**. Detection of NRPE, all-*trans*-retinal dimer (atRAL-dimer) and A2PE by HPLC analysis (C4 column). Quantitation by integrating chromatographic peak areas. DHA-PE, 1,2-didocosahexaenoyl-*sn*-glycero-3-phosphoethanolamine. Major fatty acids in egg yolk-PE are 16:0, 18:0, 18:1, 18:2, 20:4 and 22:6.

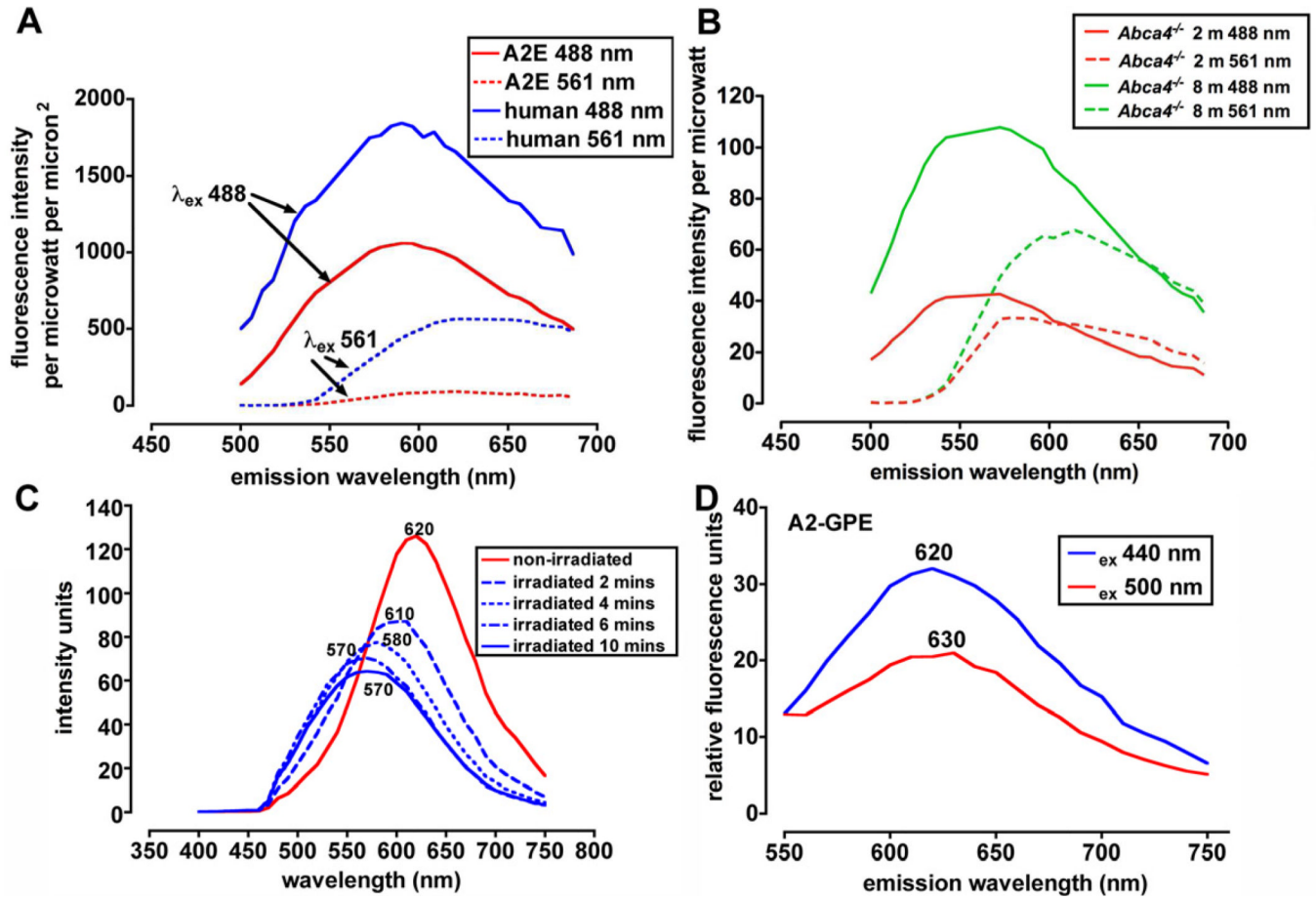

Figure 6.

Fluorescence emission spectra of RPE lipofuscin and cell-based A2E. Data recorded using confocal laser scanning fluorescence microscope (Nikon A1R MP) with a 60X objective in 6–nm increments while exciting with lasers at 488 and 561 nm. **A**. Emission spectra obtained from RPE monolayer (posterior) in cryostat sections of human eye (age 45 years) (field size 512 × 128 pixels, 0.21 um per pixel) and from A2E that had accumulated in ARPE-19 cells (field size 512 × 512 pixels, 0.42 microns per pixel). Emission data adjusted for laser power and pixel size. **B**. Emission spectra obtained from cryostat sections of eyes obtained from *Abca4* null mutant mice at ages indicated in months (m). Field size was 512 × 64 pixels, 0.09 microns per pixel. Spectra were adjusted for pixel size and laser power. **C**. Fluorescence emission of A2E (in DMSO/buffered saline) when not irradiated (red trace) and when irradiated for the times indicated (blue traces). Emission peak wavelengths are indicated adjacent to each trace. Note the decrease in peak height and the peak shift to shorter wavelengths with increasing duration of irradiation. **D**. Emission spectra of RPE bisretinoid A2-GPE (diretinal glycerophosphethanolamine). Note red-shift with increasing excitation wavelength.

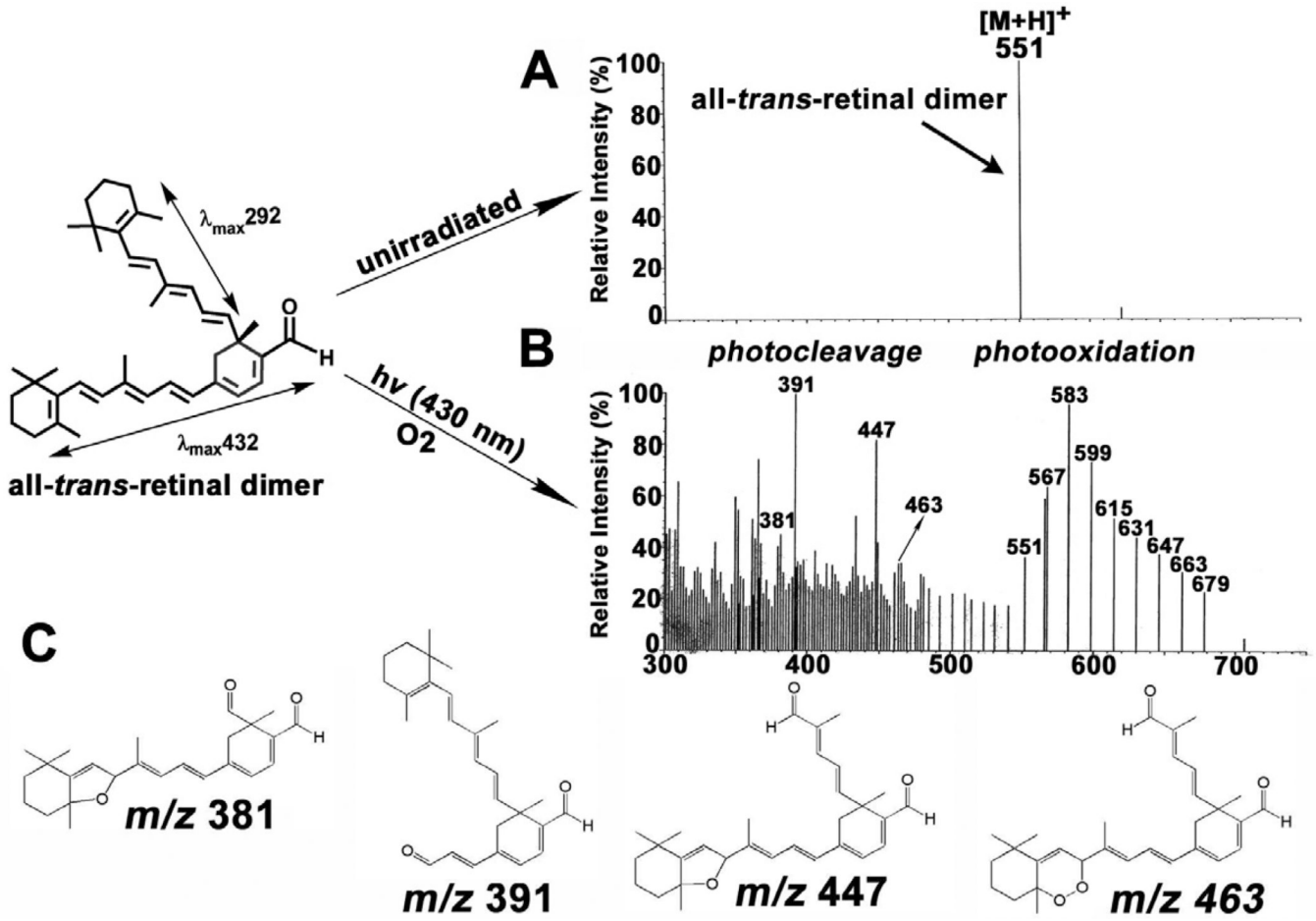

Figure 7.

Photooxidation and photodegradation of all-*trans*-retinal dimer. Analysis by electrospray ion multi-mode ionization (ESI). Samples of all-*trans*-retinal were unirradiated (**A**) or irradiated (**B**) at 430 nm (*hv*). The series of peaks from *m/z* 551–679 reflect photooxidation at carbon-carbon double bonds in all-*trans*-retinal dimer. Lower mass peaks (< *m/z* 592) correspond to all-*trans*-retinal dimer photodegradation products. **C**. Proposed structures of the largest of the photodegradation products. *Upper left*, all-*trans*-retinal dimer exhibits absorbance peaks at 432 nm and 292 nm that can be assigned to long and short arms of the molecule, respectively.

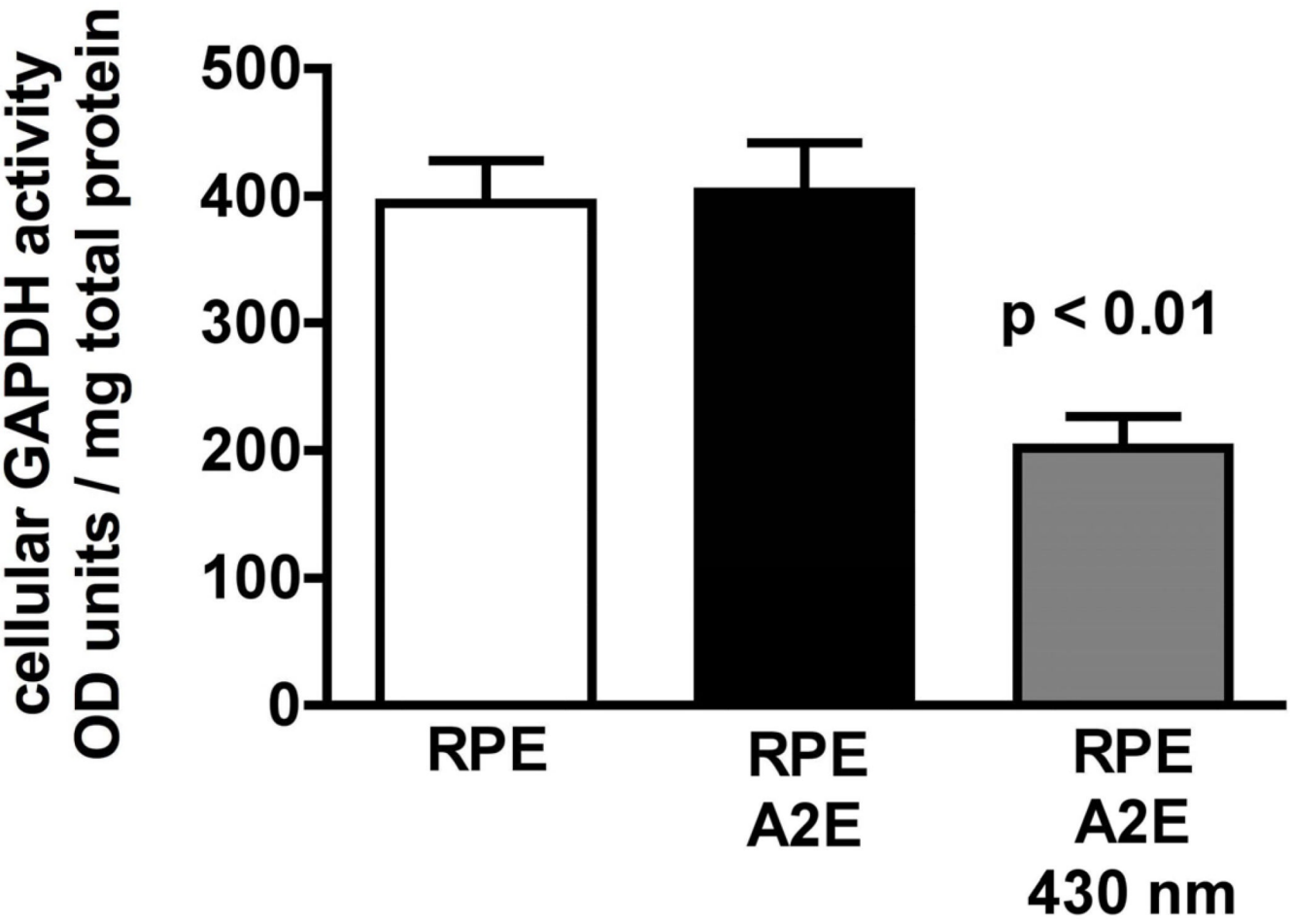

Figure 8.

Glyceraldehyde 3-phosphate dehydrogenase (GAPDH) activity is decreased in cells that have accumulated A2E and are irradiated at 430 nm (1.38 mW/cm^2). ARPE-19 cells accumulate A2E into the lysosomal compartment. With this experimental model, the incidence of cell death is not elevated in A2E-containing cells versus untreated cells.

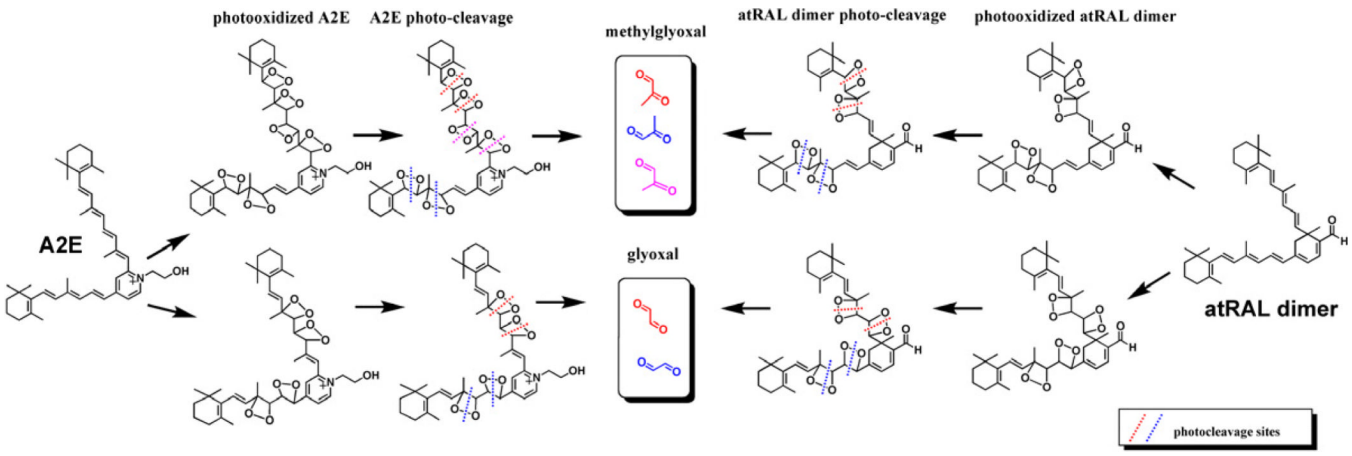

Figure 9.

Photodegradation of the RPE bisretinoids A2E and all-*trans*-retinal dimer (atRAL dimer) releases the dicerbonyls methylglyoxal and glyoxal. Potential cleavage sites at carbon-carbon double bonds are presented (dotted lines) Depending on the photodegradation patterns, each molecule of A2E and all-*trans*-retinal dimer could release 2–3 molecules of methylglyoxal or glyoxal.

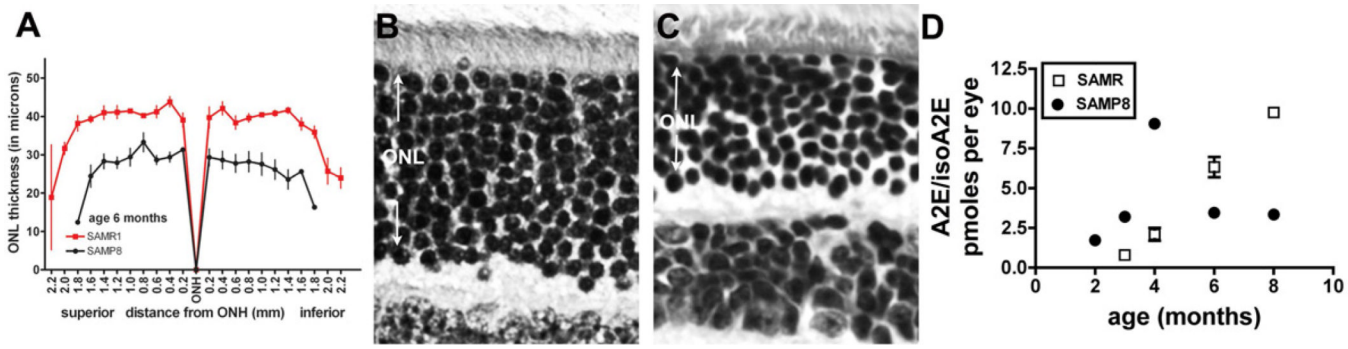

Figure 10.

Senescence accelerated mice. These mice carry the Leu450 variant in Rpe65. **A**. Quantification of outer nuclear layer (ONL) thickness in senescence-accelerated resistant (SAMR) and senescence-accelerated prone (SAMP8) mice at age 6 month. Measurements are plotted as a function of distance from the optic nerve head (ONH) in the inferior and superior hemispheres. Values are mean ± SEM of 4 eyes. **B,C**. Light micrographs of SAMR and SAMP8 central retinas, 6 months of age. RPE is not included in the micrographs. **D**. HPLC measurements of A2E and isoA2E in eyecups of SAMR and SAMP8 mice. Values are mean ± SEM of 2–7 samples, 6 eyes per sample.